UNITED NATIONS UNIVERSITY
GEOTHERMAL TRAINING PROGRAMME
Orkustofnun, Grensasvegur 9,
IS-108 Reykjavik, Iceland

Reports 2011
Number 26

RESISTIVITY STRUCTURE OF PAKA GEOTHERMAL PROSPECT IN KENYA

Raymond M. Mwakirani
Geothermal Development Company, Ltd. – GDC
P.O. Box 17700-20100
Nakuru
KENYA
rmwakirani@gdc.co.ke

ABSTRACT

The resistivity structure of the Paka prospect was studied in order to give a structural image of the underground from data taken at the surface. Electrical resistivity is strongly affected by geothermal processes. An increased fluid content due to fracturing and the development of more conductive alteration clay minerals, can give rise to electrical resistivity contrasts which, with reliable mapping, can increase the chances of discovering geothermal resources and define the extent of a geothermal reservoir. This is done through imaging the controlling structures of geothermal systems, and locating the characteristic permeable fracture zones. Due to the presence of hot rocks and saline hot waters, geothermal areas tend to have low resistivity. In this report about the Paka prospect, indications are of the existence of a high-temperature geothermal system assuming the resistivity structure is in equilibrium with the alteration mineralogy and present day rock temperatures. It is presumed that the reservoir zone, which is expected to consist mostly of resistive minerals such as chlorite and epidote, will exhibit temperatures above 230ºC.

1. INTRODUCTION

Geophysical exploration techniques are employed during surface exploration to identify structures that could be possible conduits for geothermal fluids, locate the presence of heat sources and outline drilling areas where exploration wells can be sited. The most common geophysical method employed in surface exploration for geothermal energy is the electrical conductivity technique.

The Magnetotelluric (MT) and Transient Electromagnetic (TEM) methods were used to characterize the geothermal potential of the Paka field. Geothermal resources are ideal targets for Electromagnetic methods since they produce strong variations in subsurface electrical resistivity. The MT method has been used in geothermal exploration since the early 1970s. Paka is one of the high-temperature geothermal fields within the northern rift valley in Kenya (Figure 1). A total of 107 MT and 73 TEM sites were acquired from Paka geothermal prospect. These data have been used to study the subsurface resistivity distribution of Paka geothermal field. The results are presented in the form of cross-sections and iso-resistivity maps.

2. RESISTIVITY OF ROCKS

Most rock-forming minerals are electrical insulators. Measured resistivity in the earth materials is primarily controlled by the movement of charged ions in pore fluids or by the conduction of secondary minerals. Although water itself is not a good conductor of electricity, groundwater generally contains dissolved compounds that greatly enhance its ability to conduct electricity. Hence, connected porosity and fluid saturation tend to dominate electrical resistivity together with mineral alteration. In addition to pores, fractures within crystalline rock can lead to low resistivity if they are filled with fluids. The resistivity of a material is defined as the electrical resistance in ohms (Ω) between the opposite faces of a unit cube of the material (Kearey et al., 2002). For a conducting cylinder of resistance (R), length (L) and cross-sectional area (A) the specific electrical resistivity is given by:

$$\rho = \frac{RA}{L} \qquad (1)$$

where ρ = Specific resistivity (Ωm);
R = Resistance (Ω);
A = Area (m^2);
L = Length (m).

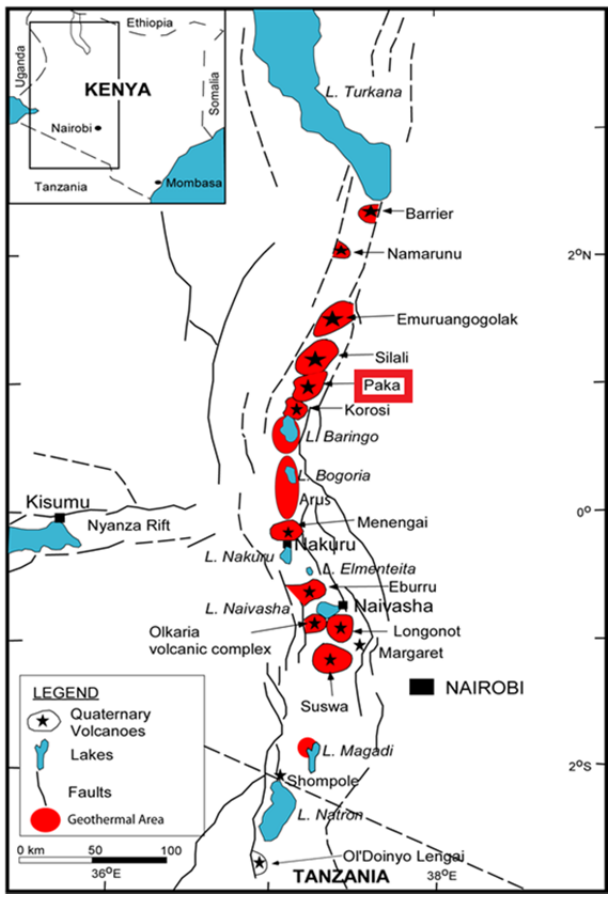

FIGURE 1: A map showing the location of Paka geothermal prospect (name shown in a red box) in the Rift valley in Kenya (modified from Ouma, 2010)

The electrical resistivity of rocks is influenced mainly by the following parameters (Hersir and Björnsson, 1991):

- Salinity of the water;
- Temperature;
- Pressure;
- Porosity and permeability of the rock;
- Amount of water (saturation);
- Water-rock interaction and alteration.

2.1 Salinity of water

The bulk resistivity of a rock is mainly controlled by water-rock interaction and the resistivity of the pore fluid which is dependent on the salinity of the fluid. An increase in the amount of dissolved solids in the pore fluid can increase the conductivity by large amounts (Figure 2). Conduction in solutions is largely a function of salinity and the mobility of the ions present in the solution. Therefore, the conductivity, σ, of a solution may be determined

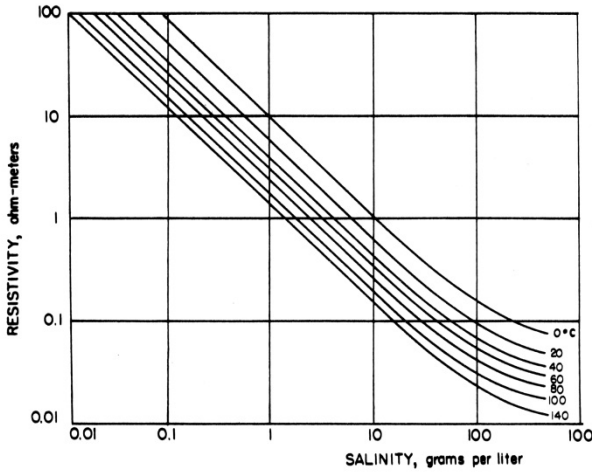

FIGURE 2: The resistivity of solutions of NaCl as a function of concentration and temperature (from Keller and Frischknecht, 1966)

by considering the current flow through a cross-sectional area of 1 m^2 at a voltage gradient of 1 V/m. This is expressed in Equation 2 (Hersir and Björnsson, 1991):

$$\boldsymbol{\sigma = {}^{1}/_{\rho} = F(c_1 q_1 m_1 + c_2 q_2 m_2 + \ldots.)} \quad (2)$$

where σ = Conductivity (S/m);
F = Faraday's number (9.65×10^4 C);
c_i = Concentration of ions;
q_i = Valence of ions;
m_i = Mobility of ions.

2.2 Temperature

At moderate temperatures, 0-200°C, the resistivity of aqueous solutions decreases with increasing temperature. This is due to an increase in ion mobility caused by a decrease in the viscosity of the water. Dakhnov (1962) has described this relationship as:

$$\rho_w = \frac{\rho_{wo}}{1 + \alpha(T - T_o)} \quad (3)$$

where ρ_w = Resistivity of the fluid at temperature T (Ωm);
ρ_{wo} = Resistivity of the fluid at temperature T_0 (Ωm);
α = Temperature coefficient of resistivity (°C), $\alpha \approx 0.023°C^{-1}$ for $T_o = 23°C$;
T_o = Room temperature.

At high temperatures, there is a decrease in the dielectric permittivity of the water, resulting in a decrease in the number of dissociated ions in the solution. This effectively increases fluid resistivity. At temperatures above 300°C, fluid resistivity starts to increase as shown in Figure 3.

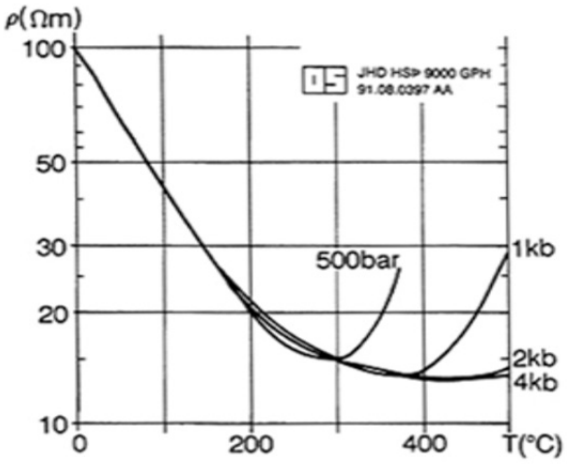

FIGURE 3: Electrical resistivity of solutions of NaCl water as a function of temperature at different pressures (Hersir and Björnsson, 1991; modified from Quist and Marshall, 1968)

2.3 Porosity and permeability of the rock

Porosity is a measure of the void spaces in a material, and is measured as a fraction, between 0 and 1, or as a percentage from 0 to 100%. More specifically, porosity of a rock is a measure of its ability to hold fluid. Permeability, on the other hand, is a measure of the ability for fluid flow through a rock. Both porosity and permeability are important for electrical conductivity of rocks.

It has been observed that resistivity varies approximately as inverse powers of the porosity when the rock is fully saturated with water. This observation has led to the widespread use of an empirical function relating resistivity and porosity known as Archie´s law, given by the formula (Archie, 1942):

$$\rho = \rho_w a \varphi_t^{-n} \quad (4)$$

where ρ = Bulk resistivity (Ωm);
ρ_w = Resistivity of the pore fluid (Ωm);

φ = Porosity expressed as a fraction per unit volume of rock;
a = Empirical parameter varies from < 1 for inter-granular porosity to slightly above 1 for rocks with joint porosity;
n = Cementing factor, usually about 2.

Permeability is a measure of how well fluids will flow through a material. Effects, like the packing, shape and sorting of granular materials, control the rock's permeability. Although a rock may be highly porous, if the voids are not interconnected, then fluids within the closed, isolated pores cannot move. The degree to which pores within the material are interconnected is known as effective porosity. Rocks such as pumice and shale can have high porosity, yet they can be nearly impermeable due to the poorly interconnected voids. The range of values for permeability in geological materials is extremely large. The most permeable materials have permeability values that are millions of times greater than the least permeable ones. Permeability is often directional in nature. Secondary porosity features, like fractures, frequently have a significant impact on the permeability of the material. In addition to the characteristics of the host material, the viscosity and pressure of the fluid also affect the rate at which the fluid will flow (Lee et al., 2006).

2.4 Water-rock interaction and alteration mineralogy

Geothermal water reacts with rocks to form secondary alteration minerals. The distribution of alteration minerals provides information on the temperature of the geothermal system and the flow path of the geothermal water. The alteration mineralogy provides information on the physicochemical characteristics of the geothermal water. The alteration intensity is normally very low for temperatures less than 50-100°C; pore fluid conduction is the main conduction mechanism in this zone. At temperatures from 100 to 220°C, low-temperature zeolites and the clay mineral smectite are formed (Árnason et al., 2000). The range where low-temperature zeolites and smectite are abundant is called the smectite-zeolite zone. In this zone the resistivity is low due to the loosely bound cations of the alteration minerals. In the temperature range from 220 to about 240-250°C, the low-temperature zeolites disappear and smectite is transformed into chlorite in a transition zone, the so-called mixed-layer clay zone, where smectite and chlorite coexist in a mixture. Mineral conduction is dominant in this zone due to the loosely bound cations. At about 250°C the smectite has disappeared and chlorite is the dominant mineral, marking the beginning of the chlorite zone. At still higher temperatures, about 260-270°C, epidote becomes abundant in the so-called chlorite-epidote zone. This zoning applies for fresh water basaltic systems. In brine systems, the zoning is similar but the mixed-layer clay zone extends over a wider temperature range, or up to temperatures near 300°C (Árnason et al., 2000).

Normally one would expect the resistivity of a geothermal system to decrease with increasing temperature. However, in high-temperature volcanic areas, the resistivity in the chlorite and chlorite-epidote alteration zone increases due to an extremely low concentration of mobile cations, a result of high-temperature alteration minerals being bound in a crystal lattice. The conduction mechanism here is surface and pore fluid conduction. Figure 4 demonstrates the relationships

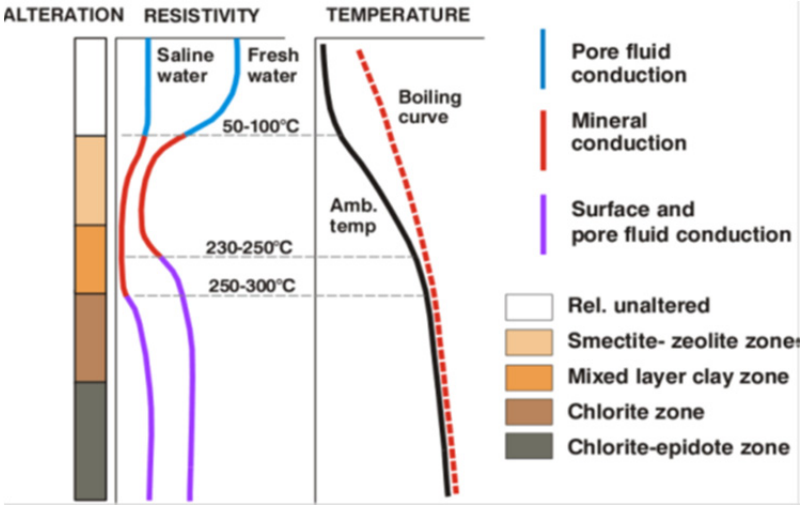

FIGURE 4: General resistivity structure of a high-temperature geothermal system showing resistivity variations with alteration and temperature (modified from Flóvenz et al., 2005)

between resistivity, alteration and temperature, both for saline and fresh water systems. At depths, where the resistivity increases below the low-resistivity zone, a chlorite alteration zone is expected, indicating a temperature of 230°C or higher, provided the alteration is in equilibrium with the temperature. If the geothermal system has cooled down, then the alteration remains the same and hence the resistivity structure is the same. In such a case, the interpretation of the resistivity structure can be misleading since it reflects alteration minerals that were formed in the past and not necessarily present day temperature. There have also been instances where alteration minerals have indicated lower temperatures than that measured in wells. This has been interpreted as being due to a young system being heated up while alteration lagged behind, so that the system is still not in equilibrium with the temperature (Hersir and Árnason, 2009).

3. OVERVIEW OF GEOPHYSICAL METHODS

Geophysical exploration methods for geothermal resources are divided into two categories according to the parameters to be measured or investigated: direct methods and structural / indirect methods. The following overview is mainly based on Hersir and Björnsson (1991).

3.1 Structural methods

Magnetic surveys. Magnetic methods in geothermal exploration are applied in mapping geological structures (structural method). The most important applications are finding the location and depth of concealed intrusives, tracing dykes and faults, locating buried lava, finding the depth to the basement, locating hydrothermally-altered areas, and evaluating paleomagnetism.

Gravity surveys. In geothermal exploration, the gravity method is used to detect geological formations with different lateral densities. Different types of rocks in the crust and mantle have different densities, hence different gravitational forces. The gravity force between two masses, m_1 and m_2, at a distance r apart, is given by Newton's law of gravitation (m_1 is the first mass and m_2 is the mass of the earth):

$$F = G\frac{m_1 m_2}{r^2} \tag{5}$$

where G = The universal gravitational constant, $G = 6.670 \times 10^{-11}$ Nm^2/kg^2.

Gravity variations are measured with a gravimeter. These are very sensitive mechanical instruments which measure the change in acceleration (g) at one place relative to another reference place (relative measurement). The unity for acceleration is m/s^2. A gravity unit (g.u.) is equal to 10^{-6} m/s^2. One g.u. is equal to 0.1 mgal. The sensitivity of gravimeters is about 0.005 mgal. Absolute gravimeters are now being developed. They are already used in the field to measure gravity at selected base stations. Their accuracy is similar to the accuracy of conventional gravimeters.

In order to obtain information about the subsurface density from gravity measurements, it is necessary to make several corrections to the measured gravity values before they can be represented in terms of geological structures. The final corrected value for the gravity anomaly is called the Bouguer anomaly, Δg_B. It can be expressed as:

$$\Delta g_B = g_m + C_{FA} - C_B + C_T - g_N \tag{6}$$

where g_M = Measured gravity corrected for tidal effects (attraction of the moon and the sun) and drift in the gravimeter;

C_{FA} = Elevation correction or free-air correction; it can be written as: $C_{FA}= 0.3086 \cdot H$, where H is the height of the station in m above sea level;

C_B = Correction for excess mass material between the station and sea level, Bouguer correction. It can be written as $C_B = 0.04191 \cdot \rho \cdot H$, where ρ is the density (g/cm^3); the density must be well known in order to be able to calculate the Bouguer correction.

C_T = Topographical correction, correction for local terrain variations near the station. It includes distortion by hills and valleys. It can be written as $C_T = \rho \cdot GL$, where *GL* is a parameter characterising the topography around the station. Topographic corrections always decrease measured gravity.

g_N = Normal reference gravity, according to an international formula. It takes into account the latitude of the station, i.e. the earth's shape (ellipsoid), and centrifugal acceleration.

Seismic surveys. Active seismic measurements involve injecting waves into the ground and recording the energy that reflects back at different times and locations on the surface using geophone receivers. Processed seismic data can give information about subsurface geology, including rock types and fault structures. It can also be correlated with gravity to define more accurate velocity models which provide more accurate depth estimates, hence, assisting in locating drilling locations. A passive seismic method makes use of naturally induced micro-earthquake activities and can be used to delineate permeable fractures acting as a flow path for geothermal fluids, delineate the brittle-ductile zone, and also to monitor useful indicators in natural or induced reservoir phase changes during exploitation of a geothermal field (see Simiyu et al., 1998).

3.2 Direct methods

Thermal methods – Thermal methods directly measure temperature and heat (temperature surveys). No other methods have such a good correspondence with the properties of the geothermal system. There are approximately four sub-categories: temperature alone (direct interpretation, mapping); geothermal gradient (vertical variation of temperature measured in soil or drillholes); heat flow (calculated from the product of gradient and thermal conductivity); heat budgets (measuring spring flow and steam output and/or integrating heat flow). Measuring the temperature alone or the geothermal gradient is of direct significance in local geothermal work, while measuring the heat flow is of more regional or global interest.

Heat can be exchanged in different ways such as by conduction (transfer of heat through a material by atomic vibration (often in steady-state)); convection (transfer of heat by motion of mass, i.e. liquid, natural circulation of hot water); and through radiation (does not play any significant role in geothermal exploration). Conduction plays a significant role in the transfer of heat in the earth's crust. Thermal convection is usually a much more effective heat transfer mechanism than thermal conduction and is most important in geothermal systems.

Electrical resistivity methods. An electrical method is either a sounding method or a profiling method, depending on what kind of resistivity structure is being investigated. The sounding method is used for mapping resistivity as a function of depth. The profiling method maps resistivity at more or less constant depth and is used to map lateral resistivity changes.

Electrical methods can be divided into the following categories and subcategories. In DC-methods, a constant current ***I*** (independent of time) is introduced into the ground through a pair of electrodes on the surface of the earth. The current creates a potential field in the earth. By measuring the electrical field ***E*** (potential difference over a short interval), the subsurface resistivity can be inferred. Schlumberger soundings, head-on profiling, dipole soundings and profiling are useful DC-methods.

In magnetotellurics (MT) and audio-magnetotellurics (AMT), fluctuations in the natural magnetic field of the earth and the induced electric field are measured. Their ratio is used to determine the apparent resistivity.

The time domain or transient electromagnetic method (TEM) is a method where a magnetic field is built up by transmitting a constant current into a loop or grounded dipole; then the current is turned off and the transient decay of the magnetic field is measured. It is used to determine the resistivity.

Measuring the electrical resistivity of the subsurface is the most powerful prospecting method in surface geothermal exploration. Resistivity is directly related to the properties of interest, like salinity, temperature, porosity (permeability) and alteration mineralogy. To a great extent, these parameters characterise a reservoir (Hersir and Björnsson, 1991). The specific resistivity, ρ, is defined through Ohm's law, which states that the electrical field strength $\boldsymbol{E}$ (V/m) at a point in a material is proportional to the current density $\boldsymbol{J}$ (A/m^2):

$$E = \rho J \tag{7}$$

The proportional constant, ρ, depends on the material and is called the (specific) resistivity and is measured in Ωm. The reciprocal value of resistivity is conductivity ($1/\rho = \sigma$). Resistivity can also be defined as the ratio of the potential difference ΔV (V/m) to the current I (A) across a material which has a cross-sectional area of 1 m^2 and is 1 m long.

$$\rho = \frac{\Delta V}{I} \tag{8}$$

The common principle of all resistivity sounding methods is to induce an electrical current into the earth and monitor signals, normally at the surface, generated by the current distribution. In conventional direct current soundings such as Schlumberger soundings, this is done by injecting current into the ground through electrodes at the surface; the signal measured is the electric field (the potential difference over a short distance) generated at the surface. In magnetotellurics (MT), the current in the ground is induced by time variations in the earth's magnetic field and the signal measured is the electric field at the surface. In transient electromagnetics (TEM), the current is also induced by a time varying magnetic field but, in this case, the source is of a controlled magnitude, generated by the current in a loop or grounded dipole and the monitored signal is the decaying magnetic field at the surface (Hersir and Björnsson, 1991).

4. ELECTROMAGNETIC METHODS USED IN PAKA GEOTHERMAL PROSPECT

In EM-methods (electromagnetics), alternating current (AC) of various frequencies or current varying with time in a controlled way, is used instead of DC-current. Many different configurations of transmitters and receivers are used. Direct contact with the ground or induction coupling characterize these methods.

Electromagnetic methods were used to investigate the subsurface resistivity in Paka geothermal field using time domain or transient electromagnetic methods (TEM) and magnetotellurics (MT). The results will be discussed and a brief introduction to the methods will be given as well.

4.1 Transient electromagnetic method (TEM)

In the central-loop transient electromagnetic method (TEM), a loop of wire is placed on the ground and a constant magnetic field of known strength is built up by transmitting a constant current into the

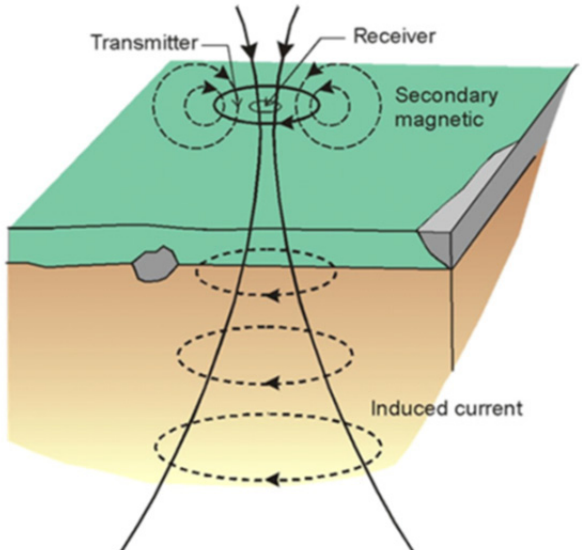

FIGURE 5: The central-loop TEM sounding configuration, showing the transmitter loop and receiver coil and the transient current flow in the ground (from Hersir and Björnsson, 1991)

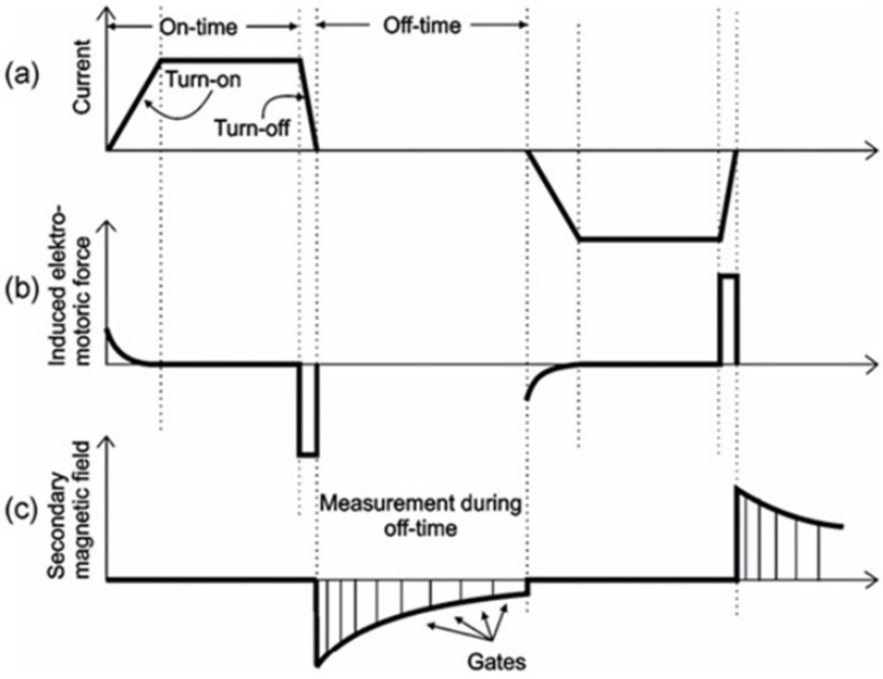

FIGURE 6: Basic nomenclature and principles of the TEM method: (a) The current in the transmitter loop; (b) Induced electromotive force in the ground; and (c) The secondary magnetic field measured in the receiver coil. For the graphs of the induced electromotive force and the secondary magnetic field, it is assumed that the receiver coil is located in the centre of the transmitter loop, the central loop configuration (Christensen et al., 2006)

loop (Figure 5). The current is then abruptly turned off (Figure 6). The decaying magnetic field induces an electrical current in the ground. The current distribution in the ground induces a secondary magnetic field which decays with time. The decay rate of the secondary magnetic field is monitored by measuring the voltage induced in a receiver coil (or a small loop) at the centre of the transmitter loop, see Figure 5.

In this work, the data were acquired using two different instruments. For TEM, a Zonge GDP-32 receiver was used. The TEM equipment used is from Zonge and consists of a current transmitter, XMT transmitter controller, GDP-32 data logger, a receiver coil with an effective area of 10,000 m^2, a 120 VA power generator, a voltage regulator and a transmitter loop. Before data acquisition, both the receiver and the transmitter controller high-precision crystals are warmed up for a period of about an hour and then synchronized to ensure that induced voltage is measured by the receiver at the correct time after current turn-off. In the field setup, a 300 m × 300 m transmitter wire loop was used and a 9 A half-duty square wave current was transmitted at frequencies 16 and 4 Hz. The transient signal was recorded in the time interval of 36.14 μs to 96.85 ms at logarithmically spaced sampling gates after current turn-off. For each frequency, several repeated transients were stacked and stored in a memory cache inside the Zonge data logger and later transferred to a personal computer for processing. For the Time Domain Electromagnetic method (TDEM, same method as the previously discussed TEM), a Phoenix V8 receiver was used and the data, at 25 Hz and 5 Hz frequencies, was stacked in a flashcard memory which was later transferred to a personal computer for processing; the universal sounding format (USF) files were then used as an input to the TemX software program (see

Árnason, 2006a). In the field set up, a 200 m by 200 m transmitter wire loop was used and a 13 A half-duty square-wave current was transmitted at frequencies 25 and 5 Hz.

The current distribution and the decay rate of the secondary magnetic field depend on the resistivity structure of the earth. The decay rate, recorded as a function of time after the current in the transmitter loop is turned off can, therefore, be interpreted in terms of the subsurface resistivity structure. The depth of penetration in the central loop TEM-sounding is dependent on how long the induction in the receiver coil can be traced in time before it is drowned in noise (Hersir and Björnsson, 1991).

The apparent resistivity, $\rho_a(t)$, for a homogeneous half-space in terms of induced voltage at late times after the source current is turned off, is given by (Árnason, 1989):

$$\rho_a(t) = \frac{\mu_o}{4\pi}\left\{\frac{2\mu_o I_o A_r n_r A_s n_s}{5t^{\frac{5}{2}}V(t,r)}\right\}^{\frac{2}{3}} \quad (9)$$

where A_r = Cross-sectional area of the receiver coil (m^2);
n_r = Number of windings in the receiver coil;
μ_o = Magnetic permeability in vacuum (H/m);
A_s = Cross-sectional area of the transmitter loop (m^2);
n_s = Number of windings in the transmitter loop;
$V(t)$ = Voltage as a function of time;
$\rho_a(t)$ = Apparent resistivity as a function of time; and
t = Time elapsed, after the transmitter current was turned off.

4.2 Magnetotelluric method (MT)

MT is an electromagnetic geophysical method used to image the earth's subsurface resistivity structure. Natural variations in the earth's magnetic field induce electric currents (or telluric currents) in the ground, dependent on the Earth's resistivity. Both magnetic and electric fields are measured on the earth's surface in two orthogonal directions. The ratio of the electric field and the magnetic field (impedance tensor) holds information about subsurface conductivity. The high frequency gives information at shallow depths while the low frequency provides information about deeper lying structures.

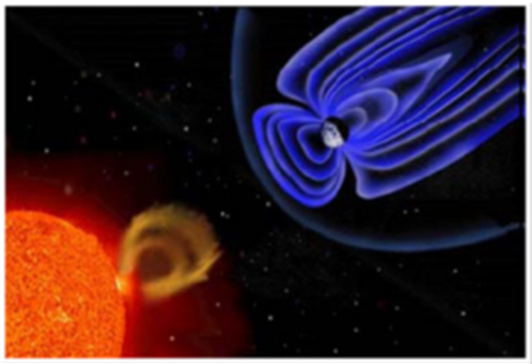

FIGURE 7: Interaction of solar wind with the magnetosphere, the source region for low frequency (< 1 Hz) natural EM fields (taken from Encyclopaedia Britannica, 2010)

At frequencies higher than 1 Hz, the EM source originates from lightning discharges in the equatorial belt while low frequencies < 1 Hz originate from the interaction between the solar wind and the earth's magnetic field, see Figure 7. These natural phenomena create MT source signals over the entire frequency spectrum (generally 10 kHz to a period of a few thousand seconds), as shown in Figure 8.

MT data acquisition is prone to a number of problems, one of them being the dead band problem. This occurs in the frequency band between 0.5-5 Hz in which natural signals are typically weak with the minimum at around 3 Hz, see Figure 8. This problem is attributable to the inductive source mechanisms, one effective below ~1 Hz and the other above ~1 Hz, which cause a reduction in data

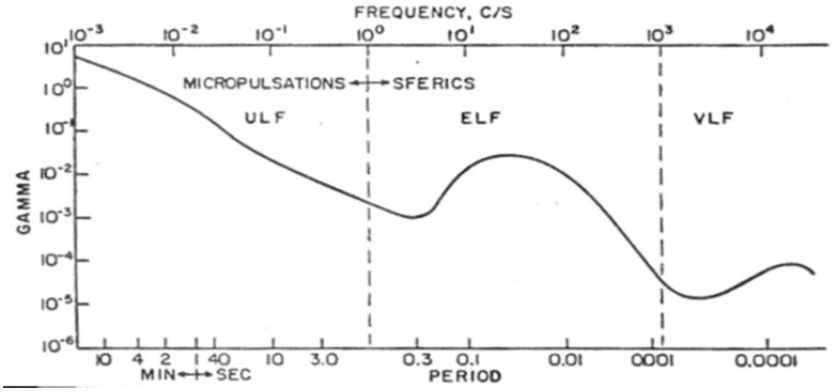

FIGURE 8: The natural magnetic field spectrum: MT "deadband" ~ 0.5-5 Hz; AMT "deadband" ~1-5 kHz

quality. Noise due to wind is also typically highest in this frequency range, thus diminishing the signal to noise ratio in the frequency band.

The data was acquired using nine sets of 5-channel MT data acquisition systems (MTU-5A) from Phoenix Geophysics. The instrumentation consisted of a data recorder, induction coils, non-polarizing electrodes, a Global Positioning System (GPS), a 12 V battery, a flash memory for data recording, and telluric and magnetic cables. The layout is made such that the electric dipoles are aligned in magnetic North-South and East-West, respectively, with corresponding magnetic channels in orthogonal directions; the third channel is positioned vertically in the ground, as demonstrated in Figure 9.

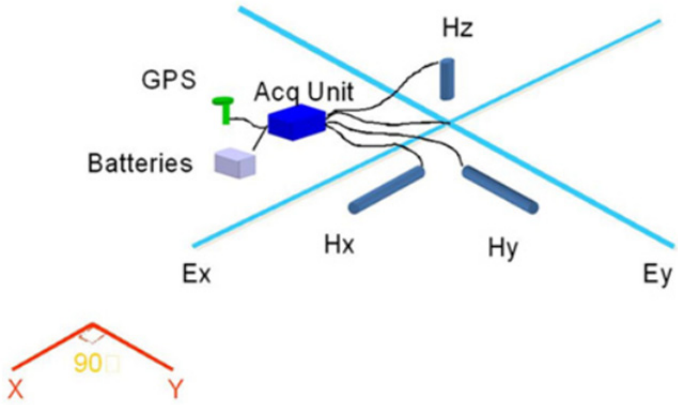

FIGURE 9: MT sounding set up (Phoenix Geophysics, 2005)

Before data acquisition, a start-up file is prepared with parameters like gains, filters, time for data acquisition and calibrations for both equipment and the coils, and is stored on a flash disk in the equipment. The ground contact resistance is generally measured to gauge the electrode coupling to the ground and a high pass filter - an anti-aliasing filter is used with a corner frequency of 0.005 Hz to remove the effect of self-potential from the electric dipoles and to prevent aliasing. The electric field was measured by lead chloride porous pots and the magnetic sensors were buried about 25 cm below the surface to minimize the wind effect and the temperature differences between day and night.

MT data were acquired for about 20 hours, giving the range from a frequency of 320 Hz and often up to a period of a few thousand seconds, which generally ensures investigation depths down to several tens of kilometres. In this survey the long period data were not achieved at most of the stations because signals were drowned in noise at low frequencies. The penetration depth of the electromagnetic wave depends on the frequency where low frequency waves have a greater depth of penetration than high-frequency waves.

All the stations were time synchronized via signals from Global Positioning System (GPS) satellites so that the time-series data were processed in combination with data acquired at the same time from the other far away stations to increase the signal to noise ratio and improve the quality of the survey results. A total of 96 MT soundings were considered for interpretation from the Paka geothermal prospect.

The MT method can explore changes in resistivity down to hundreds of kilometres, which makes it the one which has the greatest exploration depth of all the EM methods, and is practically the only method for studying resistivity deeper than a few kilometres. The depth of penetration of electromagnetic fields within the earth depends on the period and the earth's conductivity structure. The propagation

of EM fields is described by the following four sets of relationships, called the Maxwell equations, which hold true for all frequencies:

Faraday's law
$$\boldsymbol{\nabla} \times \boldsymbol{E} = -\mu \frac{\partial \boldsymbol{H}}{\partial t} \tag{10}$$

Ampéré's law
$$\boldsymbol{\nabla} \times \boldsymbol{H} = \boldsymbol{J} + \varepsilon \frac{\partial \boldsymbol{E}}{\partial t} \tag{11}$$

Gauss's law for electric field
$$div\, \boldsymbol{D} = \eta \tag{12}$$

Gauss's law for magnetic field
$$div\, \boldsymbol{B} = 0 \tag{13}$$

where $\boldsymbol{E}$ = Electrical field intensity (V/m);
$\boldsymbol{H}$ = Magnetic field intensity (T);
$\boldsymbol{J}$ = Electrical current intensity (A/m^2), and $\boldsymbol{J} = \sigma \boldsymbol{E}$
σ = Conductivity (Siemens/m); $\rho = 1/\sigma$;
μ = Magnetic permeability (H/m);
ε = Electrical permittivity (F/m);
$\boldsymbol{D}$ = $\varepsilon \boldsymbol{E}$;
$\boldsymbol{B}$ = $\mu \boldsymbol{H}$.

4.2.1 Electromagnetic induction in a homogeneous earth

The ratio of electric to magnetic field intensity is a characteristic measure of the electromagnetic properties often called the characteristic impedance (Equations 14 and 15):

$$Z_{xy} = \frac{E_x}{H_y} = \frac{i\omega\mu_0}{k} \tag{14}$$

$$Z_{yx} = \frac{E_y}{H_x} = -\frac{i\omega\mu_0}{k} \tag{15}$$

where Z_{xy}, Z_{yx} = Characteristic impedance in x and y directions;
ω = Angular frequency ($2\pi f$) where f is frequency (Hz);
μ_o = Magnetic permeability in vacuum (H/m);
$E_{x,y}$ = Electric field intensity (V/m) in x, y direction;
$H_{x,y}$ = Magnetic field intensity (A/m) in x, y direction;
k = $\sqrt{i\omega\mu_o(i\omega\varepsilon + \sigma)}$stands for the wave propagation constant;
ε = Electric permittivity (F/m);
σ = Electric conductivity.

The term, $\omega\varepsilon$, in the wave propagation constant k is much smaller than conductivity σ and can be ignored, therefore, $k \approx \sqrt{i\omega\mu_o\sigma}$, is the so-called quasi-static approximation. Putting this into Equation 14 gives:

$$Z_{xy} = \frac{E_x}{H_y} = \frac{i\omega\mu_o}{k} \approx \frac{i\omega\mu_o}{\sqrt{i\omega\mu_o\sigma}} = \sqrt{i}\sqrt{\omega\rho\mu_o} = \sqrt{\omega\mu_o\rho} \cdot e^{i\pi/4} \tag{16}$$

The phase angle by which H_y lags E_x is π/4, as explained in Figure 10. If the earth is homogeneous and isotropic, then the true resistivity of the earth is related to the characteristic impedance through the following relationship:

$$\rho = \frac{1}{\mu_o \omega}|Z_{xy}|^2 = \frac{1}{\mu_o \omega}|Z_{yx}|^2 \tag{17}$$

For a non-homogeneous earth, the apparent resistivity (ρ_a) can be defined as if the earth was homogeneous using the same formula.

In practical units for a homogeneous earth the resistivity, ρ, in the equation above can be written as:

$$\rho_a = 0.2T\,|Z|^2 = 0.2T\left|\frac{E'_x}{B'_y}\right|^2 \tag{18}$$

where E' = Electrical field (mV/km); $E' = E \times 10^{-6}$;
B' = Magnetic field (nT); $B' = B \times 10^{-9}$ and $B = \mu H$ (H in Tesla), and $\mu_o = 4\pi \times 10^{-7}$.

For a non-homogeneous earth, the apparent resistivity (ρ_a) and phase (θ_a) are functions of frequency and are defined as follows:

$$\rho_a = 0.2T\,|Z|^2 \; and \; \theta_a = \arg(Z_o) \neq 45° \tag{19}$$

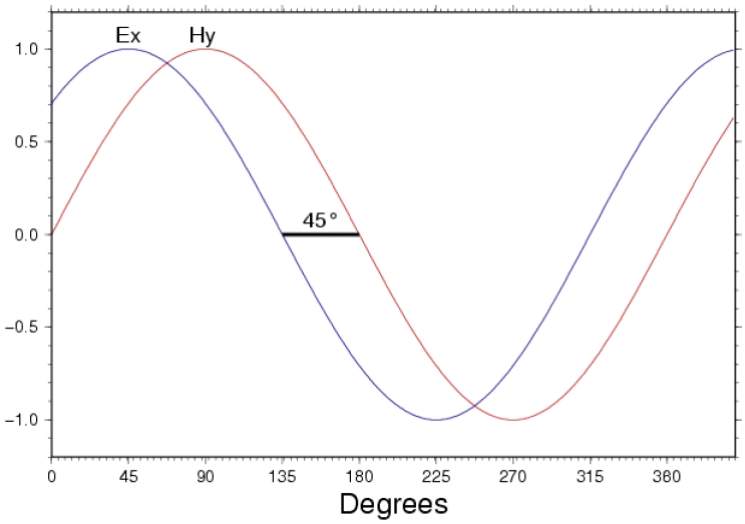

FIGURE 10: Homogeneous half space response of electrical and magnetic field describing the 45° phase difference of the E and H fields

For a 1D layered earth, conductivity varies only with depth and the diagonal elements of the impedance tensor are zero, while the off diagonal elements are equal in magnitude but have opposite signs, $Z_{xx} = Z_{yy} = 0$ and $Z_{xy} = -Z_{yx}$; in a case of a 2D earth, conductivity varies in one horizontal direction and with depth. Measuring in the electrical strike direction or after rotation in the electrical strike direction and calculating the Tipper to reveal the 90° ambiguity in geoelectric strike, $Z_{xx} = Z_{yy} = 0$ and $Z_{xy} \neq Z_{yx}$; and for a 3D earth, conductivity varies in all directions and $Z_{xy} \neq Z_{yx}$ and $Z_{xx} \neq Z_{yy}$. Theoretically, we can calculate the impedance tensor in any non-measured direction by rotating the measured impedance tensor using mathematical rotation through matrix multiplication.

As discussed above for a 1D earth the two resistivities, ρ_{xy} and ρ_{yx} should be the same. In reality, the assumption in not true; the earth is never quite 1D and the two resistivities are different. Instead of inverting for either one of them, the practice today is to invert for the rotationally invariant determinant of the tensor, which is a kind of an average of the two, independent of the measuring directions. It's given by the following equation:

$$\rho_{det} = \frac{1}{\omega\mu}|Z_{det}|^2 = \frac{1}{\omega\mu}\left|\sqrt{Z_{xx}Z_{yy} - Z_{xy}Z_{yx}}\right|^2 \; ; \; \theta_{det} = \arg(Z_{det}) \tag{20}$$

4.2.2 Skin depth

The skin depth, δ, is the depth where the electromagnetic fields have been reduced to e^{-1} of their original value at the surface. The propagation of the oscillating electromagnetic field is time dependent, that is $\boldsymbol{H}$, $\boldsymbol{E} \sim e^{i\omega t}$ and it is a vertically incident plane wave. Therefore, skin depth is used as a scale length for the time-varying field, or an estimate of how deep such a wave penetrates into the earth, and is given by:

$$\delta \approx 500\sqrt{T\rho}\,(m) \tag{21}$$

where δ = Skin depth (m);
T = Period (s); and
ρ = Resistivity (Ωm).

The formula shows that for constant resistivity, the depth of probing increases when the period T increases and decreases when the period decreases. So the depth of penetration depends on resistivity and period.

4.2.3 MT static shift

Static shift is a result of distortion of the electric field, a phenomenon produced by the presence of shallow and local bodies or hetero-geneities, see Figure 11, which are much smaller than the targets of interest and depth. These bodies cause charge distributions and induced currents that alter the magnetotelluric responses at the studied or regional scale. The term "static or telluric shift" is used because apparent resistivity is distorted by a multiplicative constant, S, and hence by a shift when presented on a log scale. This means that if not properly corrected, this can lead to very misleading interpretations. Shifts as low as $S = 0.1$ have been observed which would lead to 10 times too low resistivity values and 3 times too shallow depths to resistivity boundaries (Árnason, 2008).

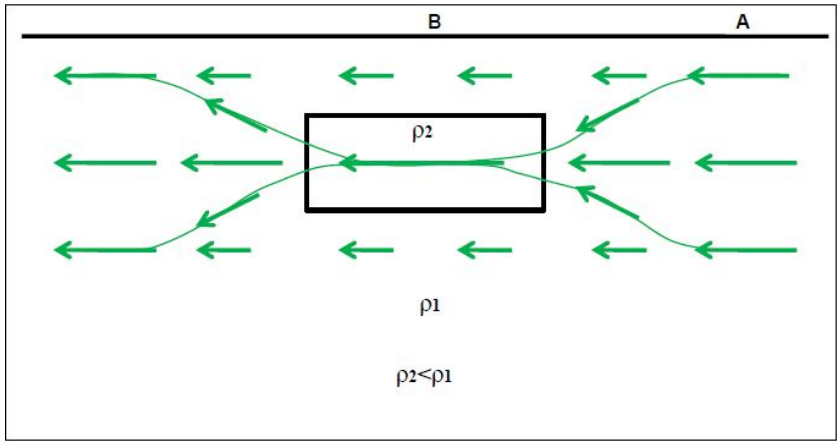

FIGURE 11: Current distortion due to conductive bodies (Sternberg et al., 1988 and Árnason, 2008)

In the case of a 1D Earth, galvanic distortion produces a constant displacement of apparent resistivity along all frequencies (Pellerin and Hohmann, 1990). This does not affect the phase. A static shift also occurs in a 2D Earth. There is no general analytical or numerical way to model the cause of static shift and thus correct it by using MT itself. Electromagnetic methods which only measure magnetic fields such as TEM do not have static shift problems that affect MT soundings (Simpson and Bahr, 2005). Therefore, TEM data can be used in conjunction with MT data from the same site in order to correct for static shifts (Sternberg et al., 1988; Árnason, 2008).

5. GEOTHERMAL PROSPECTING OF PAKA GEOTHERMAL FIELD

5.1 The resistivity survey

Paka volcano is located in the Northern rift in Kenya as shown in Figure 1. Geophysical surveys comprising of magnetotelluric (MT) and transient electromagnetic (TEM) methods were employed in an earlier survey conducted in 2007, where a total of 15 MT and 18 TEM soundings were carried out using one Phoenix MT equipment and one Zonge TEM system.

This was followed by a later survey in 2010 which brought the total number up to 107 MT and 73 TEM soundings, using a set of 8 Phoenix MT equipment and two sets of TEM systems one from Zonge systems and the other from Phoenix. The objective was to carry out a geophysical survey to establish the extent of a geothermal resource in the prospect and site wells for exploratory drilling.

The location of the transient electromagnetic (TEM) and magnetotelluric (MT) resistivity soundings that were carried out at the Paka geothermal prospect, and discussed in the present report, is shown in Figure 12.

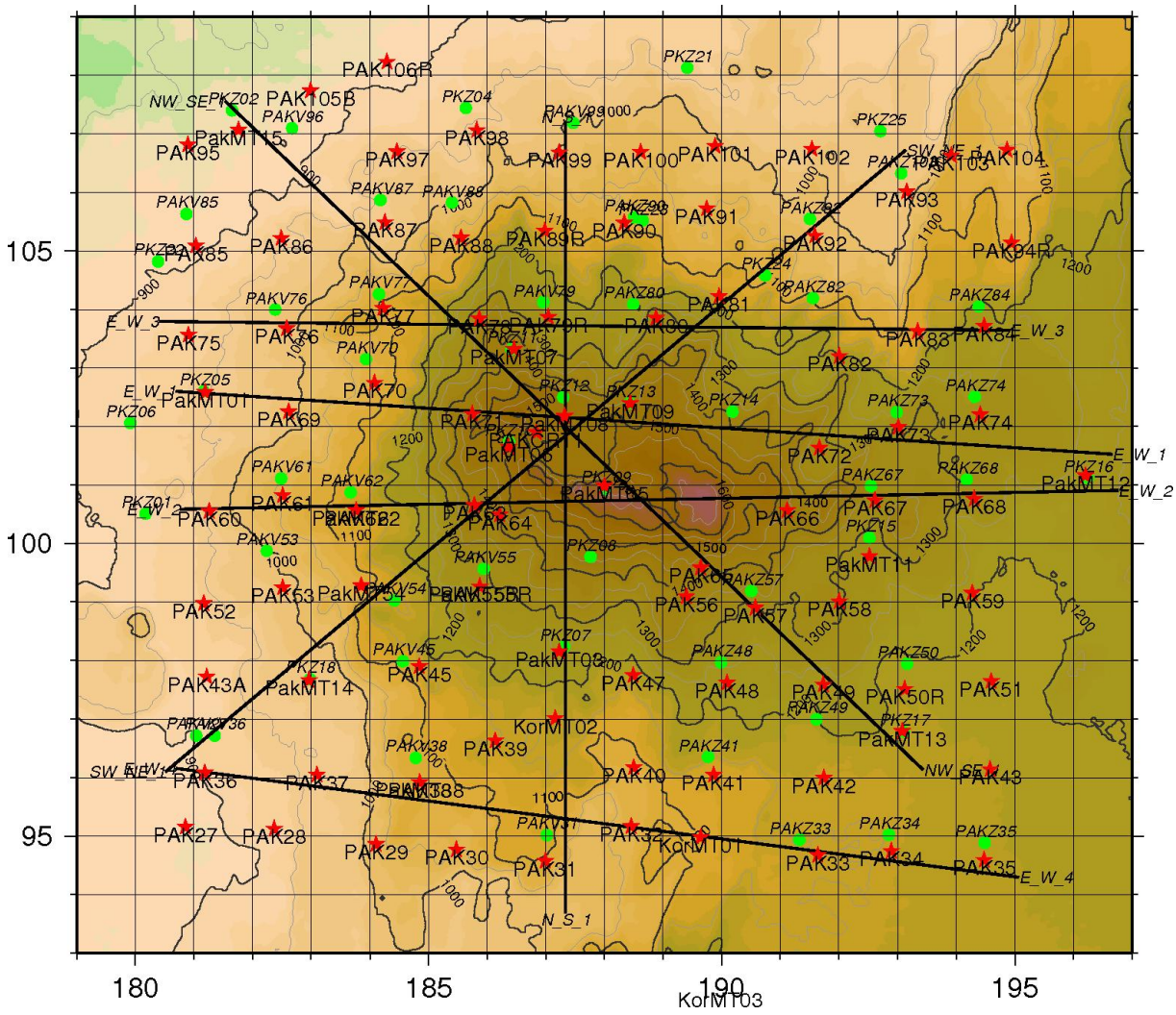

FIGURE 12: Location of TEM soundings (green dots) and MT soundings (red stars) in Paka and considered in the present report; black lines denote the location of the cross-sections used in interpreting the resistivity structure of the survey area

5.2 Geological overview of the study area

The Paka geothermal field is characterized by a well-defined volcano situated 25 km north of Lake Baringo and 15 km east of Nginyang Village. It is bound by Latitude 00°55'N and Longitude 36°12'E and rises to a maximum altitude of 1697 m with an irregular outline covering an area of approximately 280 km² (Dunkley et al., 1987). Paka is a complex multi-vent low basalt-trachyte volcano dominated by a young central caldera at the summit, which is 1.5 km in diameter. The volcano is dotted with a number of smaller satellite volcanic centres, which are linked to the main volcano by linear zones of basalt and trachyte cones and eruptive fissures.

Volcanic activity commenced by 390 ka and continued to within 10 ka BP. Trachytic pyroclastic deposits, which are seen to cover the areas around the volcano, cover much of the shield's formative lavas. The oldest exposed rocks are the Lower Trachytes, which constructed an early volcanic shield. Subsequent fracturing of the shield by the north-northeast trending faults was accompanied by eruption of the Lower Basalts from fissure sources on the eastern flanks of the volcano (Dunkley et al., 1987). The age of these sequences ranges from the early Pleistocene, represented by the shield-building trachytes, to a few hundred years BP, represented by the pristine less vegetated Young Basalts.

Surface geothermal activity is widely developed at Paka, particularly within the summit craters and the northern flanks, manifested in the form of steaming grounds and fumaroles, hot grounds, well-crystallized sulphur deposits that are locally associated with intense hydrothermal alteration and *Fimbristylisexilis* ''geothermal grass''. The main phase of faulting is aligned in a N-S direction dominated by normal faults across the volcano.

TABLE 1: Summary of the stratigraphy of Paka modified from Dunkley et al. (1993)

Young Basalts	**Age**	**Event**
Trachytes and mugearites	11 ± 3 ka	Intracaldera lavas
Pyroclastic deposits	8 ± 4 ka	Caldera formation
Upper Basalts		
Upper Trachytes		
Lower Basalts		
Lower Trachytes	219 ± 4 ka 390 ± 6 ka	Shield formation

6. PROCESSING AND INTERPRETATION OF THE PAKA GEOTHERMAL FIELD DATA

The main objective of processing is to increase the signal to noise ratio and, hence, improve the quality of the soundings and reject outliers. In this report, high quality soundings were required to give a clear understanding of the resistivity structure beneath the Paka prospect.

6.1 TEM data processing

The raw TEM data were processed by the program TemxZ, a modified version of TemX, to handle the Zonge data (Árnason, 2006a) and TemxV to handle the Phoenix V8 data, also modified from the same version of TemX. This program averages data acquired at the same frequency and calculates late time apparent resistivity as a function of turn-off time, see Figure 13. It also enables visual editing of raw data to remove outliers and unreliable data points before the data can be used for interpretation.

All the TEM soundings in the Paka prospect were interpreted by 1D (layered earth) inversion. All the TEM sounding curves and the associated 1D models are given in Appendix I (Mwakirani, 2011). The inversion was done by the Occam (minimum structure) inversion (Constable et al., 1987); an example of an inversion result is shown in Figure 13. In 1D inversion, it is assumed that the earth consists of horizontal layers with different resistivities and thicknesses. In layered inversion we invert for resistivity values as well as layer thicknesses; in Occam (minimum structure) inversion, layer thicknesses increase exponentially with depth, and we invert for resistivity values. The 1D interpretation seeks to determine the layered model where the response best fits the measured responses. When interpreting TEM resistivity, it is important to keep in mind that the depth of exploration of the TEM soundings is much greater in a resistive earth than in conductive environments. This is because the fields decay faster in conductive materials than in resistive.

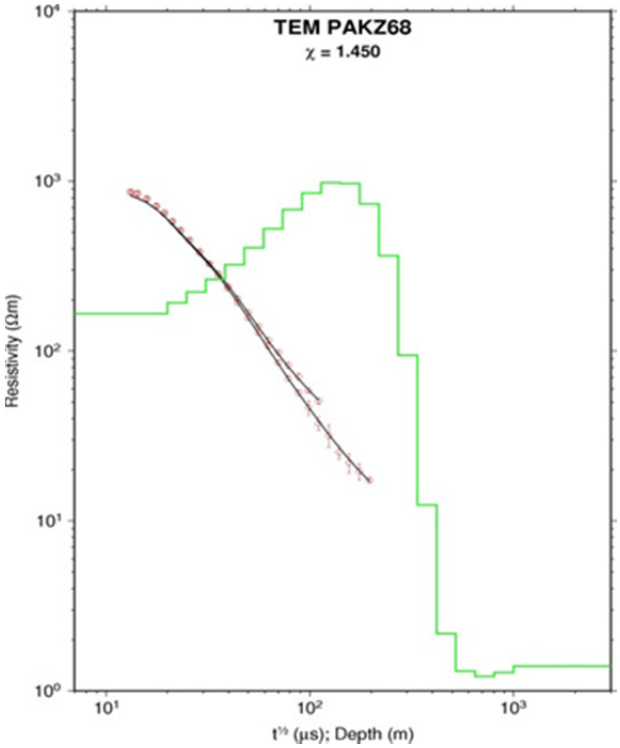

FIGURE 13: TEM sounding and 1D inversion; red circles show measured late-time apparent resistivity; the grey line apparent resistivity calculated from the model shown in green; and on top of the figure (TEM PAKZ68) is the name of the station; χ shows the fit between measured and calculated data

6.2 MT data processing

Time-series data downloaded from the MT equipment were processed by the SSMT2000 programme, provided by the equipment manufacturer, Phoenix Geophysics in Canada. First the parameter file was edited to reflect the data acquisition setup and then the resulting time-series data were Fourier transformed to the frequency domain. From the Fourier transform band, averaged cross- and auto-powers were calculated using the robust processing method; local H was used during processing, which means that the magnetic field was assumed to be noise free and the noise in the electric field was minimised. The cross-powers were then graphically edited by the MTEditor program to remove the noisy data points and evaluate "smooth" curves for both phase and apparent resistivity. The final cross- and auto powers, as well as all relevant MT parameters calculated from them (impedances, apparent resistivity and phase, coherencies, strike directions etc.) were stored in Exchangeable Data Interchange (EDI files) format and used as an input to the TEMTD program, ready for inversion. Figure 14 shows various MT parameters extracted from the EDI file. The processed data for all the MT soundings are given in Appendix II (Mwakirani, 2011).

7. INVERSION OF THE ELECTROMAGNETIC SOUNDINGS

The inversion problem is to determine the relevant physical parameters characterizing the system from the measured response and it is a probability approach to the measured data. The first step in solving the inverse problem is to know how to calculate the forward problem; therefore, it is introduced briefly using the diagram below (Figure 15). The first approach is to have a guess model and let the forward algorithm calculate the response and try to get a fit with the measured data. If the calculated response does not fit with the measured data, we give it an inversion algorithm which improves the model based

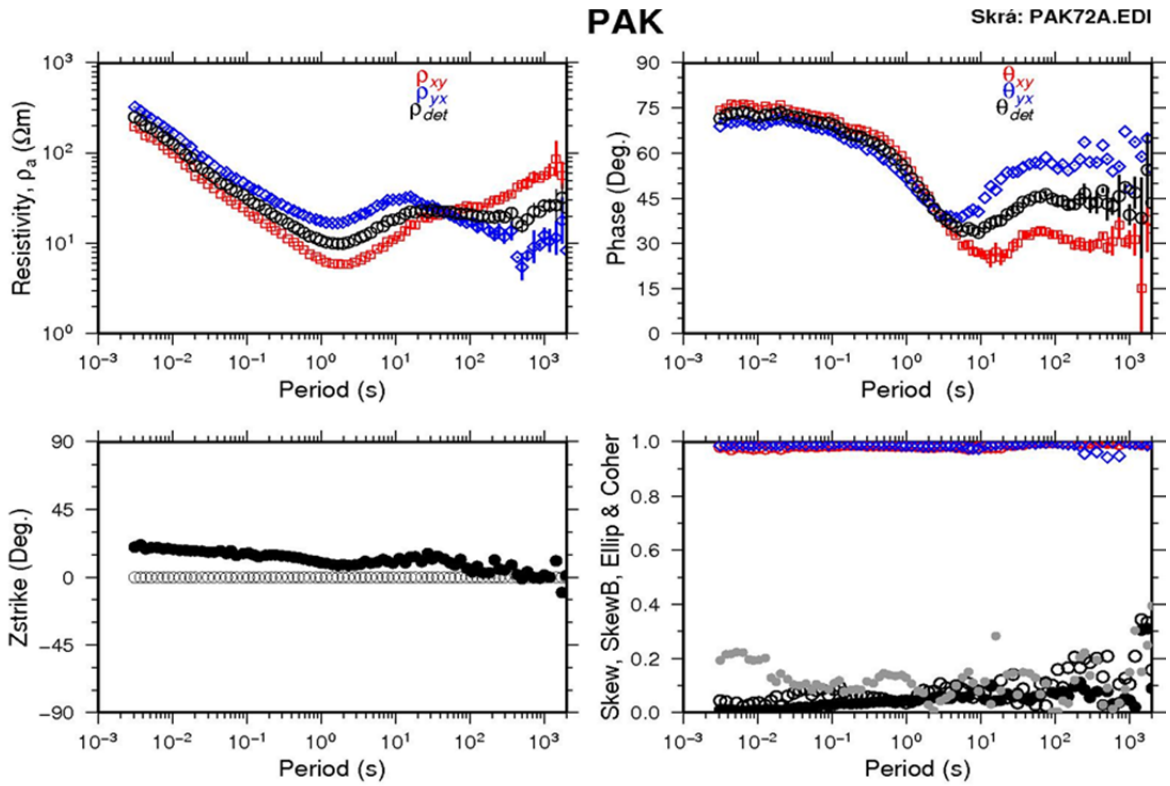

FIGURE 14: Various MT parameters extracted from the EDI file, namely the apparent resistivity, and phase in the xy and yx directions plus the one calculated from the determinant of the rotationally invariant tensor, electrical strike direction (Zstrike), coherency (measure of the data quality), skew (black dots) is a measure of 2-dimensionality, and ellipticity (grey dots)

on the misfit; this is repeated until we get the final best model which matches the model parameters of the measured data.

Forward modelling is of central importance in any inversion method and, hence, must be fast, accurate and reliable. Inversion uses forward modelling to compute the sensitivity matrix and responses for calculating the misfit. To obtain MT responses at the surface, one must solve for the electric (***E***) and magnetic (***H***) fields simultaneously via solving the second order Maxwell's Equations. The most commonly used inversion method for geoelectric soundings is the least-squares inversion method. After every iteration step we get a sensitivity matrix which places us near the exact model; this is characterized by the reduction in chi-square (χ).

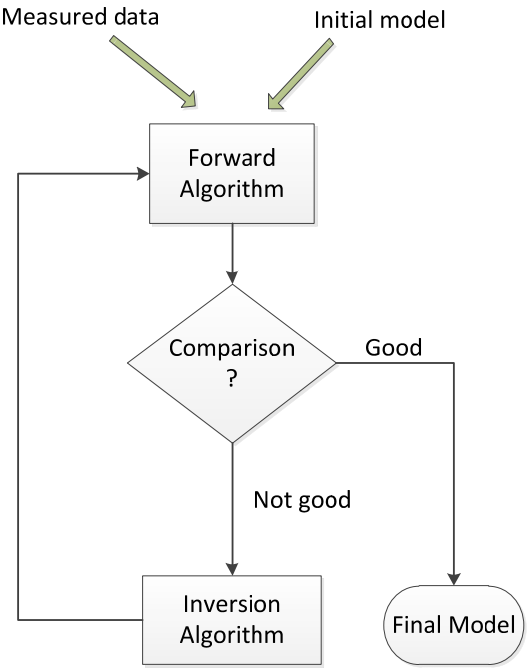

FIGURE 15: Diagram showing the sequence of the inversion process

7.1 1D inversion by TEMTD

The program TEMTD was used to perform 1D inversion of MT data. The program was written by Knútur Árnason at ÍSOR (Árnason, 2006b). The program can do 1D inversion of TEM and MT data separately and jointly. The program can invert MT apparent resistivity and/or phase derived from either of the off-diagonal elements of the MT

tensor (xy and yx modes), the rotationally invariant determinant or the average of the off-diagonal elements. In joint inversion, one additional parameter is inverted for (in addition to the layered model parameters), namely a static shift multiplier needed to fit both the TEM and MT data with the same model. The program can do both standard layered inversion (inverting for resistivity values and layer thicknesses) and Occam (minimum structure) inversion with exponentially increasing layer thicknesses with depth. It offers a user specified damping of first (sharp steps) and second order derivatives (oscillations) of model parameters (logarithm of resistivity and layer thicknesses).

The inversion algorithm used in this program is the non-linear, damped, least-squares inversion (Árnason, 2006b). The misfit function is the root-mean-square difference between measured and calculated values (χ), weighted by the standard deviation of the measured values.

Initial application of MT was based on 1D interpretation for which many inversion codes are well developed and being used (Constable et al., 1987). The MT method for imaging crustal and upper mantle conductivity has found increasing use in both geophysical exploration and large scale tectonic studies.

7.2 TEM and MT joint inversion

The joint 1D inversion of TEM and MT soundings was designed to solve the static shift problem in MT data in a volcanic environment like in Paka. The TEMTD software used offers several options of inversion of TEM and MT data, separately or jointly. For this case, they were jointly inverted.

A joint 1D Occam inversion was performed for the rotationally invariant determinant apparent resistivity and phase of the Paka soundings and the associated TEM soundings. The 1D model from the joint inversion of all the TEM and MT soundings is given in Appendix III (Mwakirani, 2011). Figure 16 shows the result of such an inversion. The best estimate of the shift parameter for this MT sounding is S = 1.39 (upper right hand corner of the apparent resistivity panel); the MT apparent

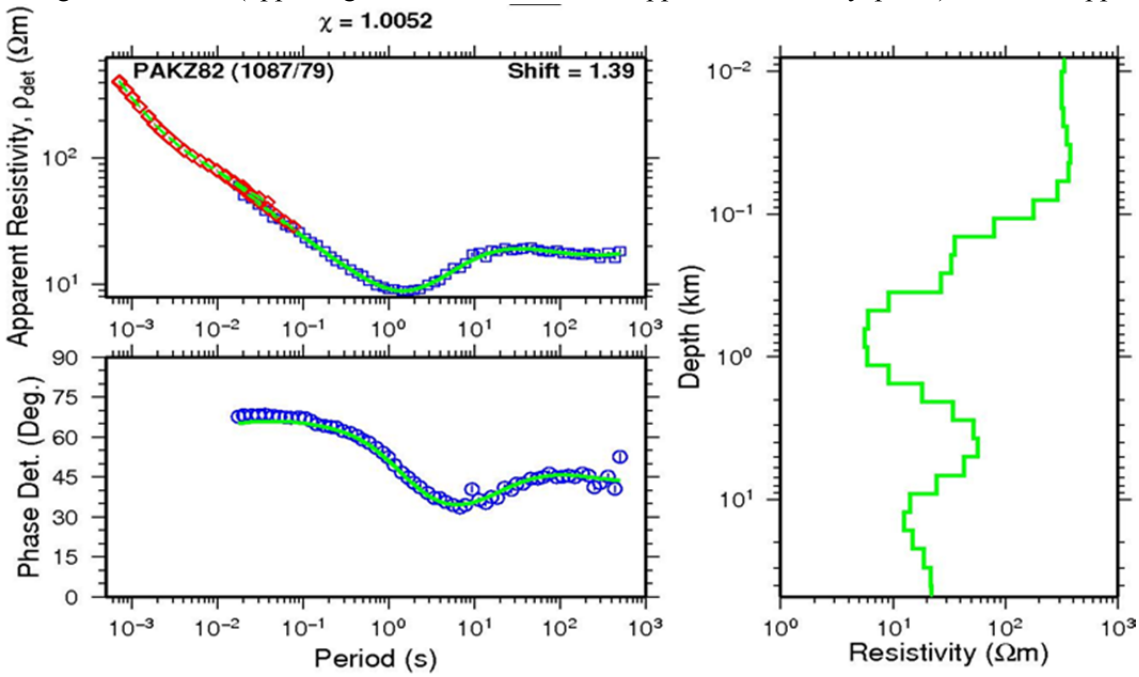

FIGURE 16: Joint 1D inversion of TEM and MT soundings; red and blue symbols on the top left panel represent the apparent resistivity from TEM and MT soundings, respectively; the bottom panel shows the apparent phase from the determinant of the MT impedance tensor; the right panel shows the results of the 1D resistivity inversion model. The green line is the fit of TEM and MT data and the phase responses

resistivity has to be divided by 1.39 to be consistent with the TEM sounding. In Figure 16, the TEM data are plotted as a function of the period (T) by using the transformation $T = t/0.2$ (Sternberg et al., 1988) and not as a function of the square root of time (t) as in Figure 13.

7.3 MT static shift analysis in PAKA prospect

The best static shift parameters for MT data were determined after joint inversion with the TEM data, then extracted from the jointly inverted models and plotted to show the spatial distribution around the prospect area. From Figure 17, it is evident that most of the MT tensors were shifted down or had shifts of less than one, an indication of near surface inhomogeneities which led to galvanic distortion.

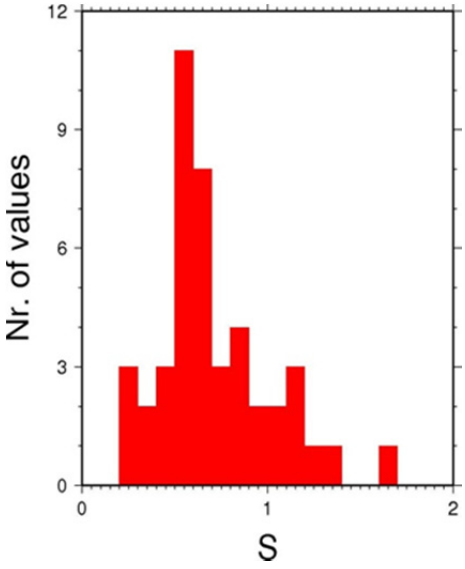

FIGURE 17: A histogram of the shift parameters for determinant apparent resistivity in the Paka prospect

In this report, 92 MT tensors were used but only 49 MT tensors had pairs for joint inversion with TEM data. The remaining MT tensors were inverted with static shift values extracted from the gridded static shift map, Figure 18, which is based on the spatial distribution of shifts extracted from the matching pairs of MT and TEM, which may not be correct as static shifts can vary from one sounding location to another, leading to errors in interpretation. The spatial distribution of static shifts is more localized at every sounding location and is not representative of the nearest station, due to the rough topography around the prospect making near surface current gather in valleys, hence reducing the current's density on ridges and mountains. The solution to this was measuring TEM data at every MT

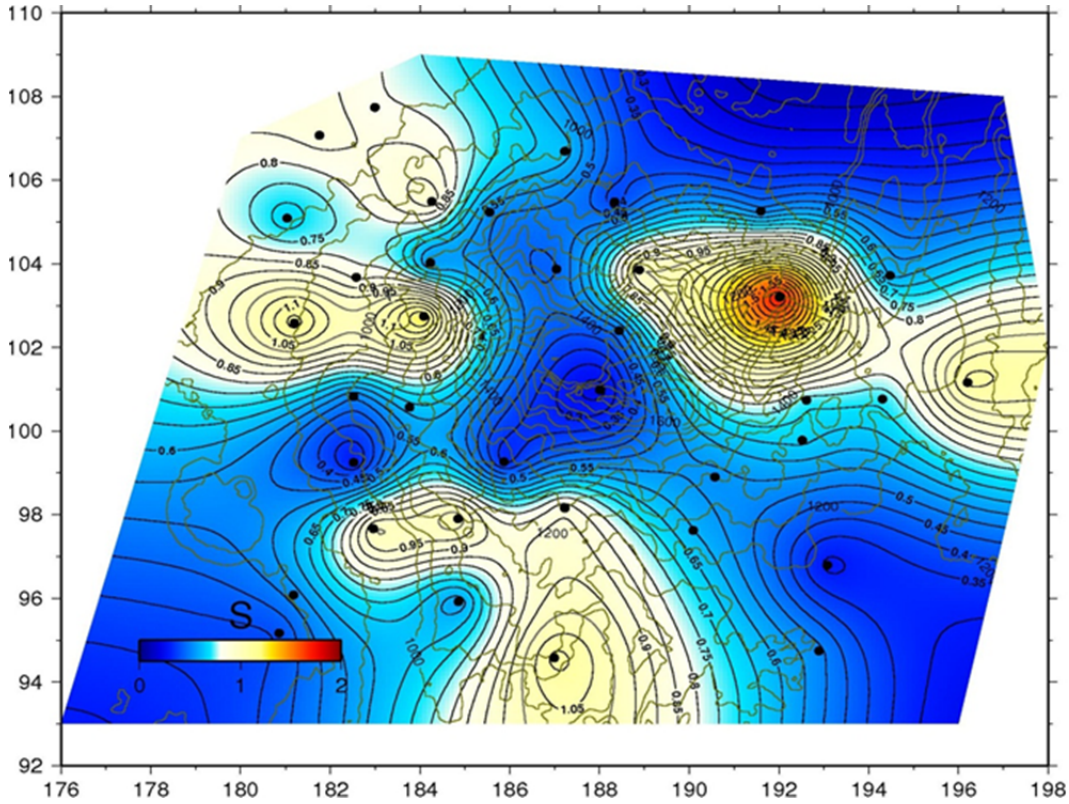

FIGURE 18: Spatial distribution of static shift parameters for determining apparent resistivity in the Paka prospect

site. In this report, the effect of static shift on MT impedance tensors was demonstrated in one cross-section by using MT tensors that were corrected by using the spatial distribution of the scaling factor in the Paka prospect.

7.4 Strike analysis

Rose diagram for the electrical strike direction based on the Tipper strike at 0.001-1 (shallow depths) and 1-1000 (greater depths) seconds are shown in Figures 19 and 20, respectively. They give information about the 2D resistivity structure regarding in which direction the resistivity changes the least; often it is the same direction as the geological strike direction as well as the direction of subsurface fractures, and is often related to high permeability, showing the flow path of the geothermal fluid. The electrical strike direction is found by minimizing the diagonal elements of the impedance tensor, Z_{xx} and Z_{yy}. However, there is a 90° ambiguity in the geoelectric strike which has been resolved by measuring H_z and calculating the Tipper. The strike is a function of frequency and is therefore different for different depths, as shown in the figures.

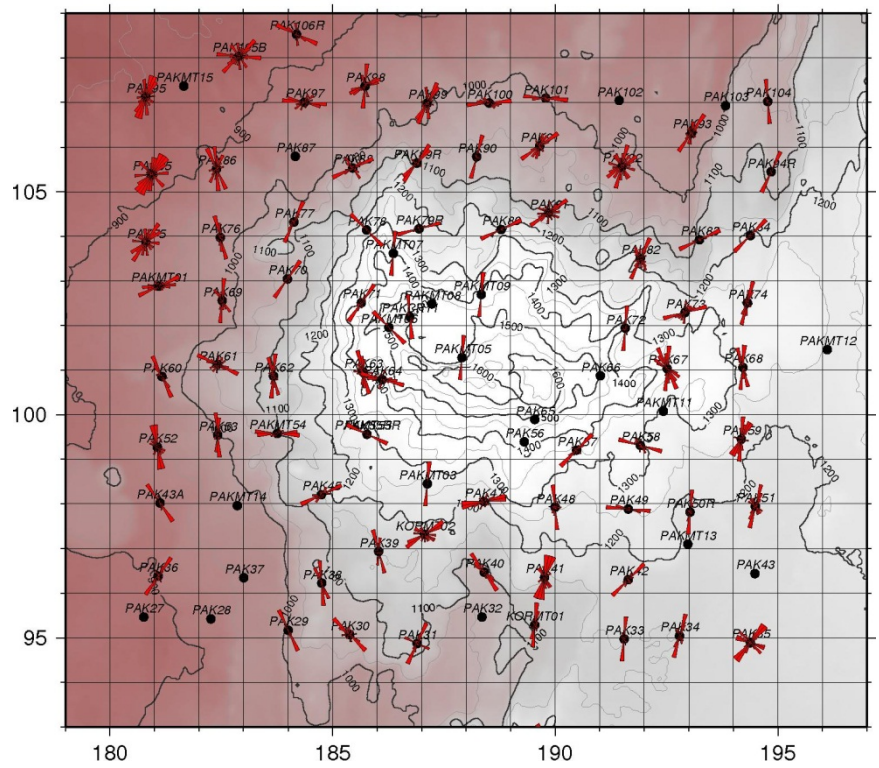

FIGURE 19: Rose diagram for the electrical strike direction based on the Tipper strike at 0.001-1 s (high frequency)

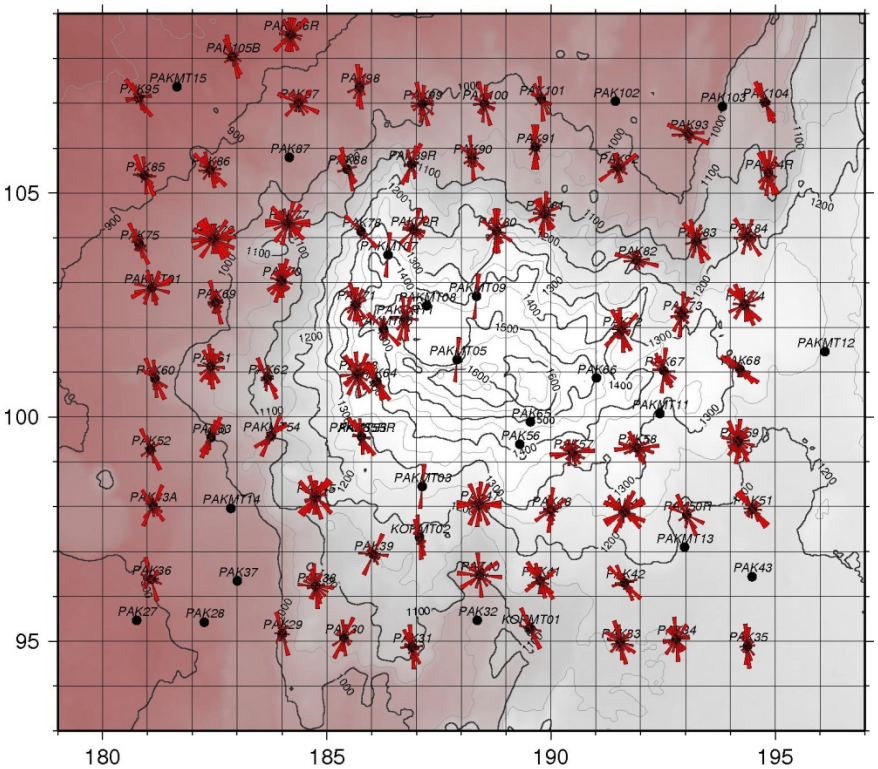

FIGURE 20: Rose diagram for the electrical strike direction based on the Tipper strike at 1-1000 s (low frequency)

8. RESULTS AND DISCUSSION

The inversion results in this report are presented in the form of selected cross-sections and iso-resistivity maps. A complete set of all the iso-resistivity maps and cross sections is published in a special report with the appendices (Mwakirani, 2011).

8.1 Cross-sections

Resistivity cross-sections were plotted from results obtained from 1D inversion by a program called TEMCROSS (Eysteinsson, 1998), developed at ÍSOR – Iceland GeoSurvey. The program calculates the best lines between the selected sites on a profile, and plots resistivity isolines based on the 1D model generated for each sounding. It is actually the logarithm of the resistivity that is contoured so the colour scale is exponential, but the numbers at contour lines are resistivity values.

Several vertical cross-sections were made throughout the survey area and their locations are shown in Figure 12. In the cross-sections, the MT soundings that were shifted based on the geospatial distribution of static shifts were included in some sections in order to demonstrate the errors they can have on the interpretation of the resistivity structure. They were not included in generating the iso-resistivity maps which made it possible to understand the general trend of resistivity in the Paka prospect without the contamination of static shifts.

The cross-sections show a typical resistivity structure of a high-temperature field: a high-resistivity layer near the surface due to un-altered formations; underlying this is low resistivity as a result of alteration minerals like smectites and zeolites; this is underlain by a high-resistivity core below where chlorite and epidote dominate and give an indication of high temperatures at depth.

Cross-section NW_SE_1 is shown in Figure 21. High resistivity of about 100 Ωm is seen near the surface which is a result of un-altered formations near the surface. Below this is a low-resistivity anomaly of less than 10 Ωm, an indication of alteration minerals like smectite and zeolites, which result from hydrothermal alteration down to about 1000 m depth (below the surface) and a temperature

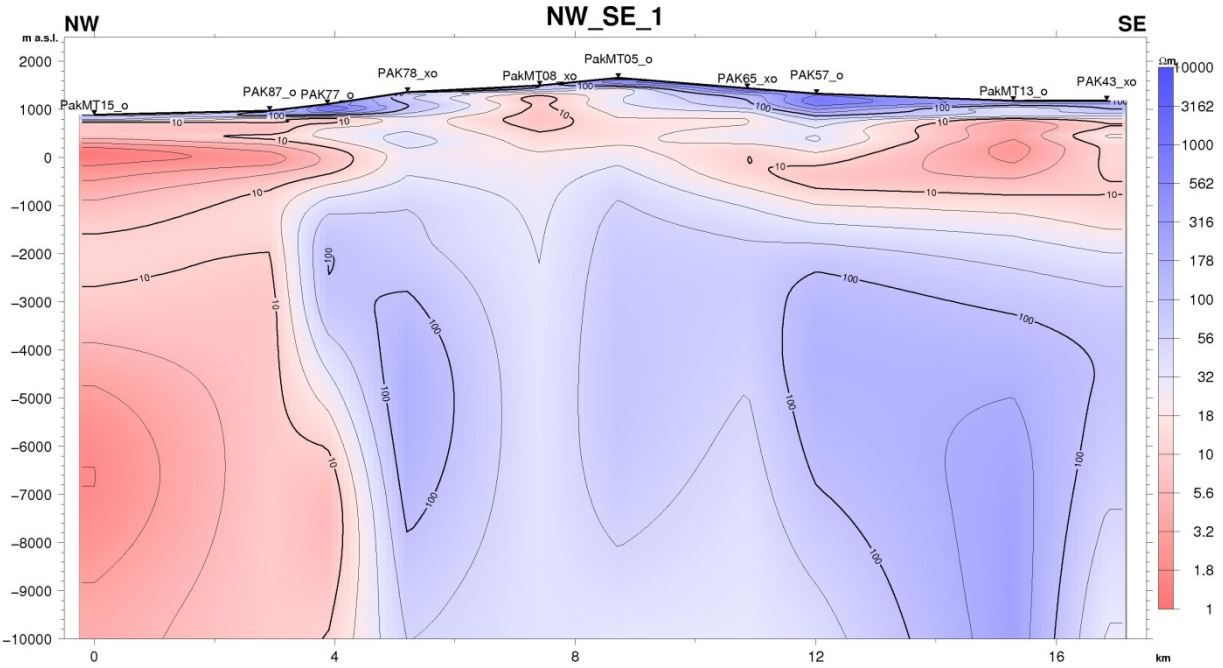

FIGURE 21: Resistivity cross-section *NW_SE_1* in the Paka prospect based on 1D joint inversion of TEM and MT data

range of 100-230°C. In the western part of the cross-section, low resistivity persists to a very great depth similar to what is observed on the resistivity maps. This is not a result of geothermal activity, but is a common trend in the East African rift system and is not clearly understood, according to Knútur Árnason (pers. commun.), who cited examples from Longonot to the south of Paka prospect. Below the low-resistivity layer, a high-resistive zone appears at depth; this layer is due to high-temperature alteration minerals such as chlorites and epidote. It defines the geothermal system from this level at 1500 m depth to about 8000 m b.s.l. It stretches directionally towards the eastern part of the prospect.

Cross-section SW_NE_1 is shown in Figure 22; it intersects profile *NW_SE_1* in Figure 21 around the Paka crater, which is the area of interest. This profile shows a similar pattern as the one seen in Figure 21. A high-resistivity layer is observed near the surface (> 100 Ωm) overlying a low-resistivity layer (< 10 Ωm) which consists of conductive clays, a result of hydrothermal alteration leading to the formation of smectites and zeolites. Below this is a high-resistivity layer of about 100 Ωm which represents the high-temperature alteration minerals, chlorites and epidote. This is the zone where the geothermal system for this prospect is defined and persists to greater depths, to about 8,000 m below sea level. The conductive zone on the western part, as explained earlier, is observed but is not considered related to any geothermal activity. The low resistivity at depth in the eastern part of the cross-section could indicate a deep conductor. This will be discussed later.

Cross-section E_W_1 is shown in Figure 23; it cuts through the Paka crater in a west-east direction and cuts perpendicular to the geologic strike, which is oriented in a NNE-SSW direction, so it gives a good image of resistivity change across the major geological structures in the prospect area. In this profile, the same resistivity structure dominates. On the western part, the conductive zone is still evident; this has been discussed in the other profiles. Here we also see low resistivity at depth in the eastern part which could indicate a deep conductor as in the *SW_NE_1* profile.

Cross-section E_W_2 is shown in Figure 24. This profile also shows a similar resistivity pattern as the ones discussed earlier, a high-resistivity layer is seen near the surface due to un-altered formations; underlying it is a low-resistivity layer representing the alteration of smectites and zeolites; below that is a high-resistive core where chlorites and epidote are dominant. At depth, a conductive zone in the

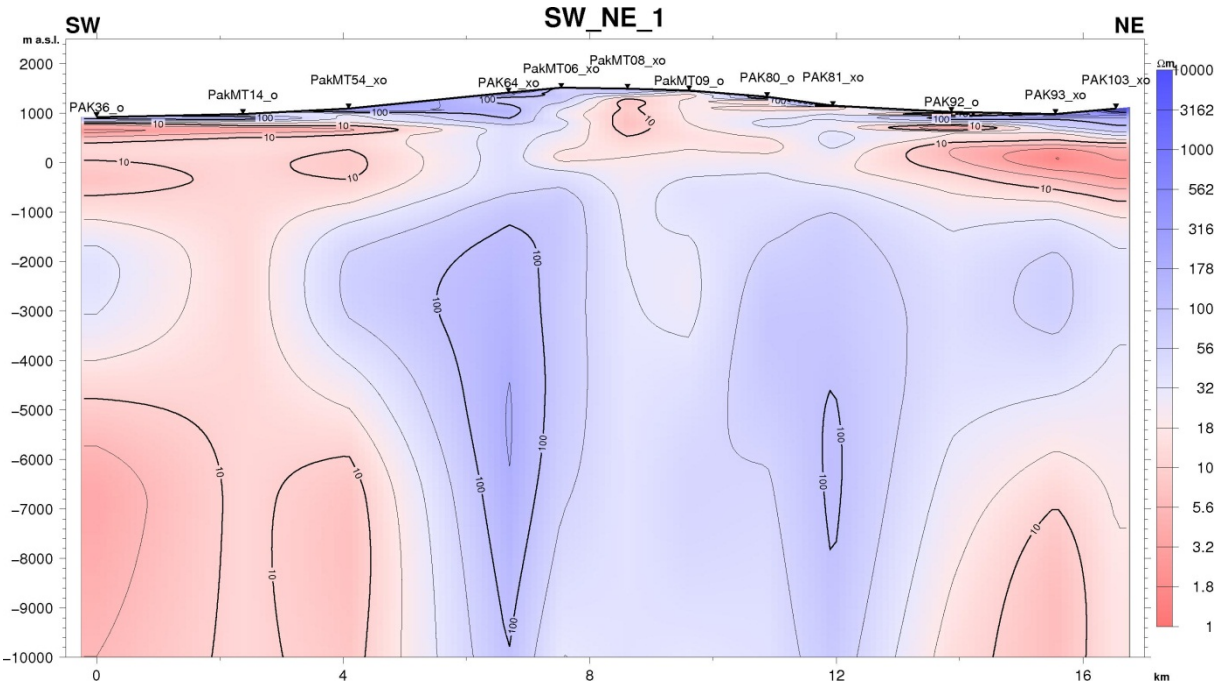

FIGURE 22: Resistivity cross-section *SW_NE_1* in the Paka prospect based on 1D joint inversion of TEM and MT data

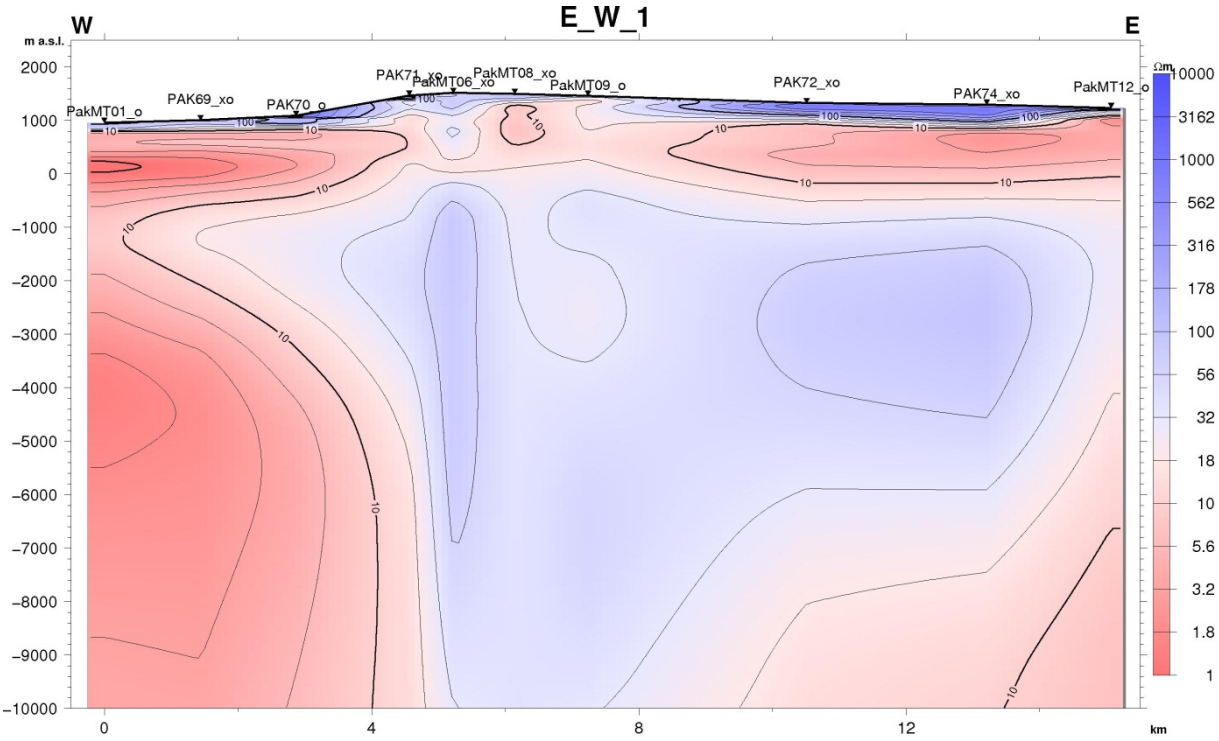

FIGURE 23: Resistivity cross-section *E_W_1* in the Paka prospect based on 1D joint inversion of TEM and MT data

eastern part is observed, as mentioned for cross-sections *SW_NE_1 and E_W_1*. Here it is more prominent as also displayed in the iso-resistivity maps. Below PAK66, the low resistivity appearing at shallower depths could be interpreted as a possible fracture zone in the profile. This, however, is not the case since the static shift of the MT sounding was estimated using the gridded map for static shift distribution. According to the observed resistivity structure, one can see that the postulated fracture zone is erroneous. This implies that the estimated static shift parameter was wrong, underlining the

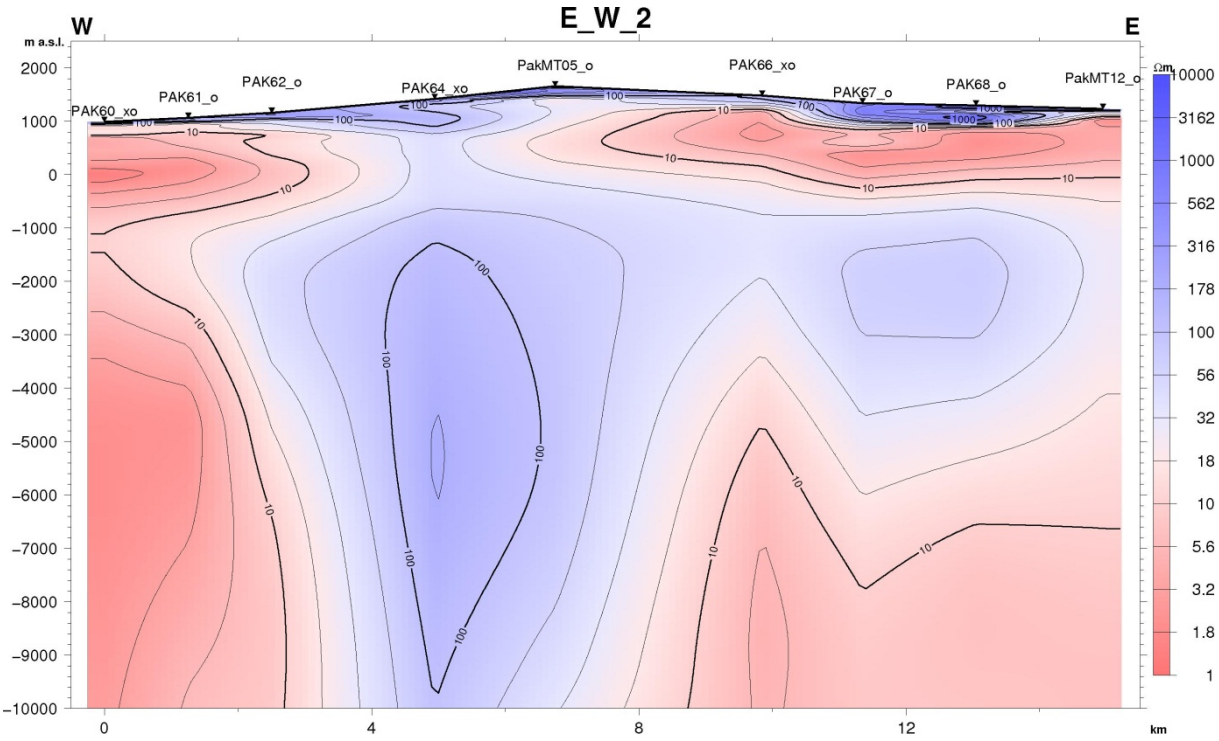

FIGURE 24: Resistivity cross-section *E_W_2* in the Paka prospect based on 1D joint inversion of TEM and MT data

importance of doing a TEM sounding at every MT site, simply because the static shift factors are localized and show very large variations. This can also be used to explain that static shift in MT tensors persists in all frequencies.

8.2 Iso-resistivity maps

The programme TEMRESD developed at ÍSOR – Iceland GeoSurvey (Eysteinsson, 1998) was used to generate iso-resistivity maps at different elevations from the 1D Occam models. The resistivity is contoured and coloured in a logarithmic scale. The elevation of the Paka prospect is generally about 1600-1700 m a.s.l. at the highest point of the massif and about 1000 m a.s.l. at the lowest points.

In this report, iso-resistivity maps are presented from 1100 m a.s.l. down to 8,000 m b.s.l., with the iso-maps reflecting the TEM resistivity structures in the uppermost 1 km, followed by MT resistivity imaging at greater depths due to the good resolution of MT soundings with depths up to tens of kilometres. In the iso-resistivity maps, MT soundings that were not corrected for static shifts were not included in generating the maps.

Resistivity map at 1100 m a.s.l. is shown in Figure 25 and represents a depth of around 300 metres below the surface on the eastern part of the map, and the near surface on the western part due to differences in elevation. A high-resistivity anomaly is dominant, with values of about 100 Ωm, an indication of un-altered formations near the surface; in the middle part of the plot, a low-resistivity anomaly is seen as an indication of the top of the resistivity cap, aligning itself in a NW-SE direction below the Paka massif.

Resistivity map at sea level is shown in Figure 26. In the central part a high-resistivity anomaly aligns itself in a NE-SW direction at about 1500 m depth; this represents the top of the high-resistivity core. Northwest and southeast of the high-resistivity core, the low-resistivity cap is clearly observed. But the low-resistivity anomaly on the western part is not well understood, as discussed in Section 8.1.

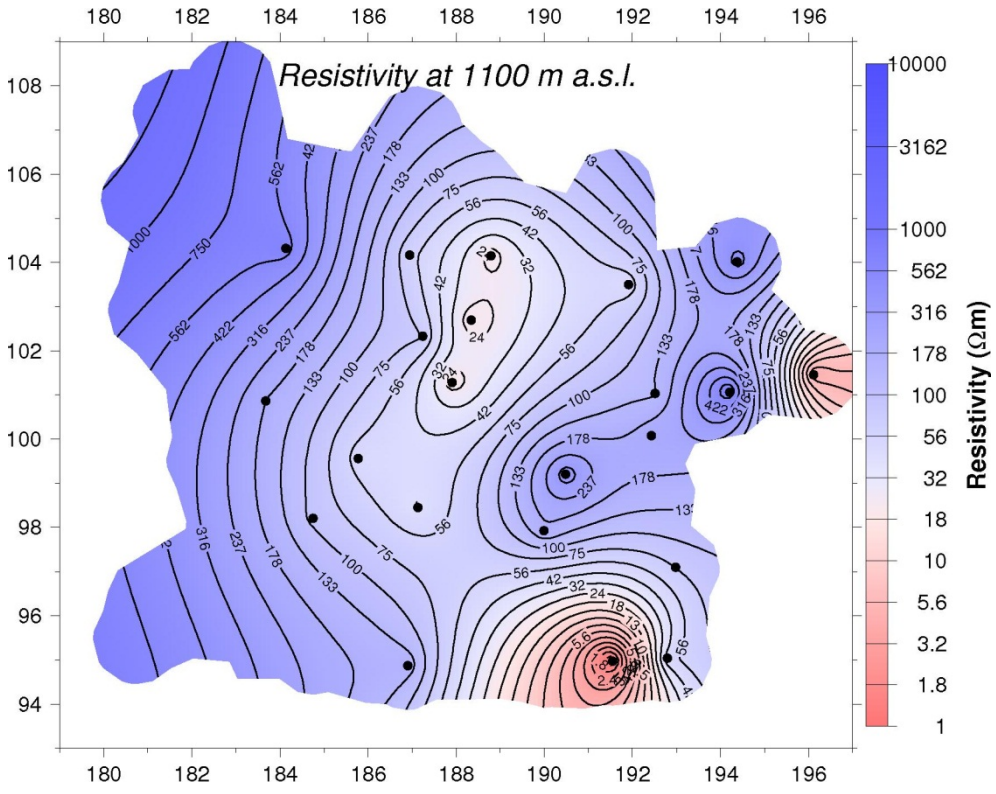

FIGURE 25: Resistivity in the Paka prospect at 1100 m a.s.l.; black dots denote MT soundings

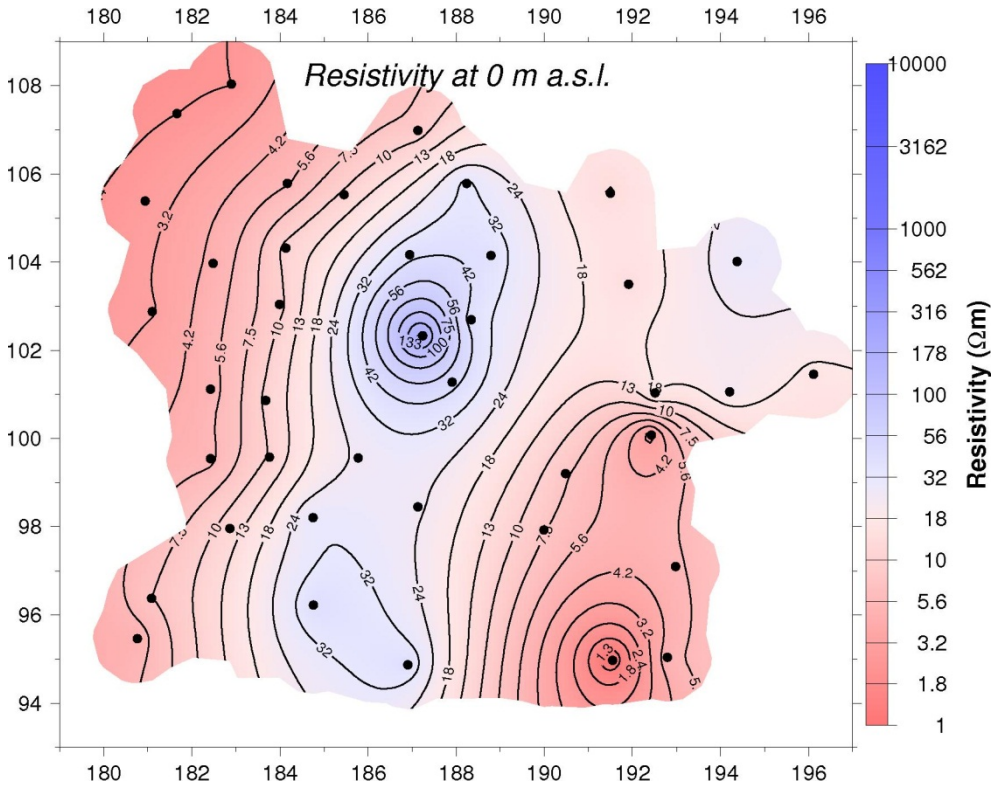

FIGURE 26: Resistivity in the Paka prospect at sea level; black dots denote MT soundings

Resistivity map at 500 m b.s.l. is shown in Figure 27. In the central part of the plot, a high-resistivity anomaly aligns itself in a NE-SW orientation and clearly delineates the geothermal system in the Paka prospect at that depth. This high-resistivity anomaly extends to greater depths, as shown in similar trends in Figures 28 and 29, which show the resistivity at 2000 m b.s.l. and 5000 m b.s.l., respectively.

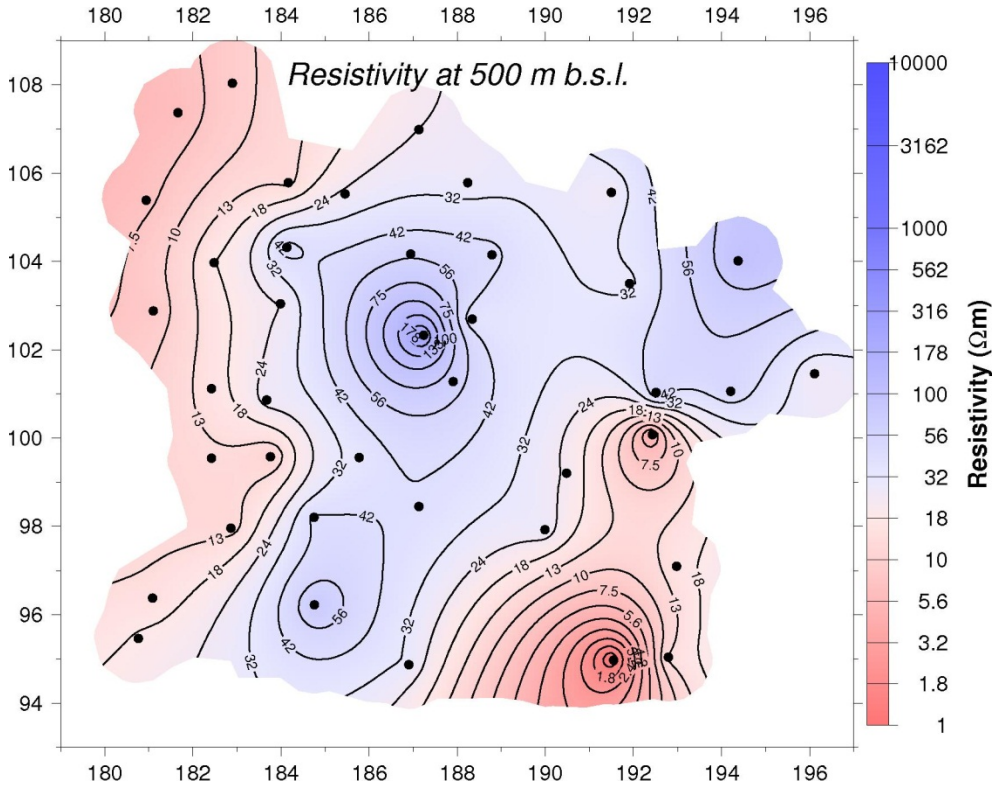

FIGURE 27: Resistivity in the Paka prospect at 500 m b.s.l.; black dots denote MT soundings

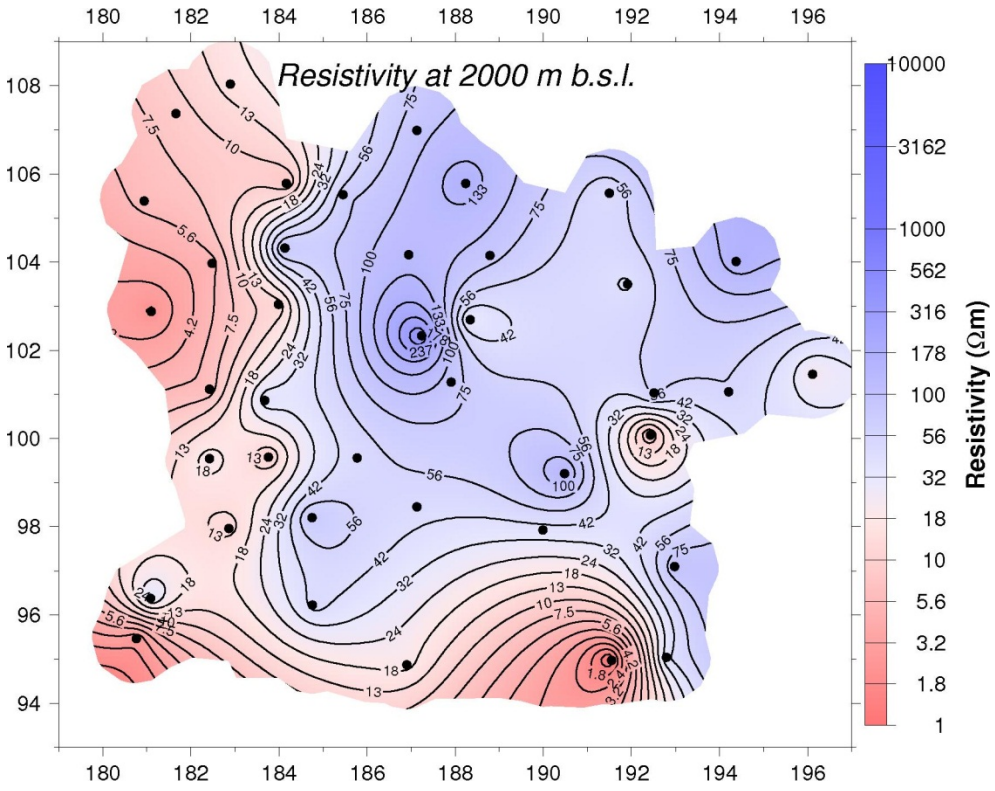

FIGURE 28: Resistivity in the Paka prospect at 2000 m b.s.l.; black dots denote MT soundings

This is due to high-temperature alteration minerals, such as chlorites and epidote, which persist at great depth in this geothermal system as seen in the cross-sections.

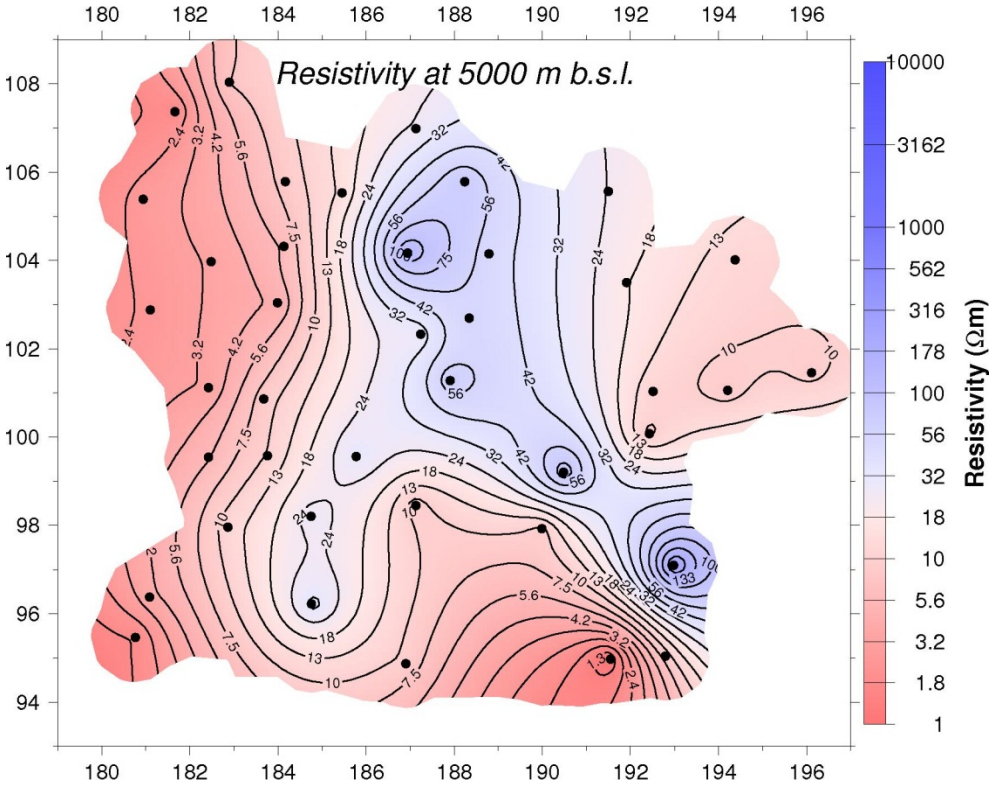

FIGURE 29: Resistivity in the Paka prospect at 5000 m b.s.l.; black dots denote MT soundings

Resistivity map at 8000 m b.s.l. is shown in Figure 30. A low-resistivity anomaly appears in the central part of the plot, below the Paka massif. This is an indication of a deeper conductor which may be related to the heat source of this geothermal system. This becomes clearer with depth, implying a deep-seated heat source. This low-resistivity may also be an indication of partial melts at depth.

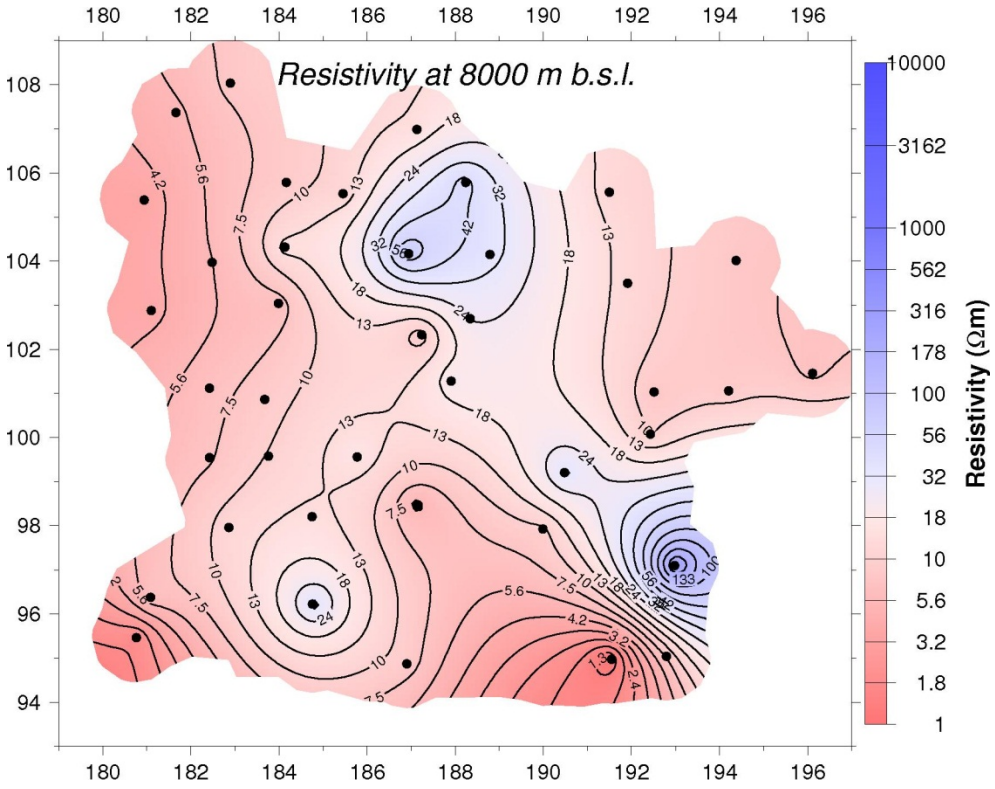

FIGURE 30: Resistivity in the Paka prospect at 8000 m b.s.l.; black dots denote MT soundings

9. CONCLUSIONS AND RECOMMENDATIONS

From the results of the joint inversion of MT and TEM data, the following resistivity layers exist as seen in the cross-sections:

1) A shallow high-resistivity layer near the surface (> 100 Ωm) which is a layer of un-altered formations about 300 m thick; the conduction mechanism is pore fluid conduction.
2) This is followed by an 800 m thick low-resistivity layer (< 10 Ωm) which consists of alteration minerals such as smectites and zeolites, formed by hydrothermal alteration; mineral conduction dominates in this zone.
3) A high-resistivity anomaly follows (> 100 Ωm) where the resistivity is dominated by the resistive high-temperature alteration minerals chlorite and epidote. Through this layer the geothermal system is defined in the depth interval about 1500-8000 m below the surface.
4) A low-resistivity anomaly representing a deep conductor appears at depth, possibly related to the heat source.

The size of the geothermal system, as outlined in Figure 27, and in terms of aerial coverage of the high-resistivity core, is estimated to be about 80 km^2. It can also be inferred that if there exists temperature equilibrium in the alteration mineralogy as seen in the resistivity profiles under the present conditions of the reservoir, then the high-resistive core hosts temperatures in excess of 230°C. This has been confirmed by gas geothermometer measurements which were carried out in the prospect but are not presented in this report.

It is recommended that more TEM data should be collected at the same sites as the MT locations in order to correct for the static shift in MT tensors, to refine the resistivity image of the prospect area and to map better the extent of the geothermal system.

ACKNOWLEDGEMENTS

I would like to express my gratitude to the UNU-GTP and the Government of Iceland for awarding me this scholarship to participate in the six months training programme. Special thanks go to Dr. Ingvar Birgir Fridleifsson, the director, Mr. Lúdvík S. Georgsson, the deputy director, Ms. Thórhildur Ísberg, Mr. Ingimar G. Haraldsson and Mr. Markús A.G. Wilde, and all of UNU staff for their coordination of the training activities and for being available to give guidance and help whenever I needed it. I am sincerely grateful to you all. My supervisor, Mr. Knútur Árnason, was always there for me whenever I needed his advice and tirelessly guided me throughout this research work and shared with me lots of valuable knowledge. My sincere appreciation goes to my other supervisor, Mr. Gylfi Páll Hersir, for his tireless guidance throughout the specialised training and project work and to Ragna Karlsdóttir for reading through my work and giving a positive contribution – thanks a lot.

I am grateful to my employer, the Geothermal Development Company Ltd. – GDC, for providing the data used in this study and for granting me leave to undertake this course. Special thanks to my colleagues at the geophysics office for their support through data collection - I thank you so much for your support. To the 2011 UNU fellows, I say thank you very much for the wonderful time and discussions that we shared together. To my beloved family, words are not enough to express my sincere thanks to you for enduring my absence, for your love and prayers throughout my entire stay in Iceland. May God bless you all.

REFERENCES

Archie, G.E., 1942: The electrical resistivity log as an aid in determining some reservoir characteristics. *Tran. AIME, 146,* 54-67.

Árnason, K., 1989: *Central-loop transient electromagnetic sounding over a horizontally layered earth*. Orkustofnun, Reykjavík, report OS-89032/JHD-06, 129 pp.

Árnason, K., 2006a: *TemX Short manual*. ÍSOR – Iceland GeoSurvey, Reykjavík, internal report, 17 pp.

Árnason, K., 2006b: *TEMTD, a programme for 1D inversion of central-loop TEM and MT data. Short manual*. ÍSOR – Iceland GeoSurvey, Reykjavík, internal report, 17 pp.

Árnason, K., 2008: *The magneto-telluric static shift problem*. ÍSOR – Iceland GeoSurvey, Reykjavík, report ISOR-08088, 17 pp.

Árnason, K., Karlsdóttir, R., Eysteinsson, H., Flóvenz, Ó.G., and Gudlaugsson, S.Th., 2000: The resistivity structure of high-temperature geothermal systems in Iceland. *Proceedings of the World Geothermal Congress 2000*, *Kyushu-Tohoku, Japan,* 923-928.

Christensen, A., Auken, E., and Sørensen, K., 2006: The transient electromagnetic method. *Groundwater Geophysics, 71*, 179-225.

Constable, S.C., Parker, R.L., Constable, C.G., 1987: Occam's inversion: a practical algorithm for generating smooth models from electromagnetic data. *Geophysics, 52,* 289–300.

Dakhnov, V.N., 1962: Geophysical well logging. *Q. Colorado Sch. Mines, 57-2*, 445 pp.

Dunkley, P.N., Smith, M., Allen, D.J., and Darling, W.G., 1987: *The geothermal activity and geology of the northern sector of the Kenya Rift Valley*. BGS Research report SC/93/1.

Encyclopaedia Britannica, 2010: *Solar wind*. Encyclopaedia Britannica Online, webpage: *www.britannica.com/EBchecked/topic/1589681/Solar-Dynamics-Observatory.*

Eysteinsson, H., 1998: *TEMMAP and TEMCROSS plotting programs*. ÍSOR – Iceland GeoSurvey, unpublished programs and manuals.

Flóvenz, Ó.G., Spangenberg, E., Kulenkampff, J., Árnason, K., Karlsdóttir, R. and Huenges E., 2005: The role of electrical conduction in geothermal exploration. *Proceedings of the World Geothermal Congress 2005, Antalya, Turkey,* CD, 9 pp.

Hersir, G.P., and Árnason, K., 2009: Resistivity of rocks. *Paper presented at "Short Course on Surface Exploration for Geothermal Resources", organized by UNU-GTP and LaGeo, Santa Tecla, El Salvador*, 8 pp.

Hersir, G.P., and Björnsson, A., 1991: *Geophysical exploration for geothermal resources. Principles and applications*. UNU-GTP, Iceland, report 15, 94 pp.

Keary, P., Brooks, M., and Hill, I., 2002: *An introduction to geophysical exploration.* Blackwell Scientific Publications, Oxford, 262 pp.

Keller, G.V., and Frischknecht, F.C., 1966: *Electrical methods in geophysical prospecting.* Pergamon Press Ltd., Oxford, 527 pp.

Lee Lerner, K., Lerner, B.W., and Cengage, G., 2006: *Porosity and permeability.* World of Earth Science, webpage*: www.enotes.com/earth-science/*

Mwakirani, R.M., 2011: *Appendices to the report "Resistivity structure of Paka Geothermal prospect in Kenya."* UNU-GTP, Iceland, report 26, appendices, 133 pp.

Ouma, P.A., 2010: Geothermal exploration and development of the Olkaria geothermal field. *Paper presented at "Short Course V on Exploration for Geothermal Resources", organized by UNU-GTP, GDC and KenGen, at Lake Bogoria and Lake Naivasha, Kenya,* 16 pp.

Pellerin, L., and Hohmann, G.W., 1990: Transient electromagnetic inversion: A remedy for magnetotelluric static shifts. *Geophysics*, 55-9, 1242-1250.

Phoenix Geophysics, 2005: *Data processing User Guide*. Phoenix Limited, 3781 Victoria Park Avenue, unit 3, Toronto, ON Canada M1W 3K5.

Quist, A.S., and Marshall, W.L., 1968: Electrical conductances of aqueous sodium chloride solutions from 0 to 800°C and at pressures to 4000 bars. *J. Phys. Chem., 72,* 684-703.

Simpson, F., and Bahr, K., 2005: *Practical magnetotellurics.* Cambridge University Press, Cambridge, UK, 254 pp.

Simiyu, S.M., Oduong, E.O., and Mboya, T.K., 1998: *Shear wave attenuation beneath the Olkaria volcanic field*. KenGen, internal report.

Sternberg, B.K., Washburne, J.C., and Pellerin, L., 1988: Correction for the static shift in magnetotellurics using transient electromagnetic soundings. *Geophysics, 53,* 1459-1468.